Available online at www.sciencedirect.com
SCIENCE DIRECT®
Journal of Sound and Vibration 276 (2004) 807–836
JOURNAL OF SOUND AND VIBRATION
www.elsevier.com/locate/jsvi

# Dynamic analyses of plane frames by integral equations for bars and Timoshenko beams

H. Antes*, M. Schanz, S. Alvermann

*Institute of Applied Mechanics, Technical University Braunschweig, Spielmannstr. 11, D-38106 Braunschweig, Germany*

Received 5 March 2003; accepted 5 August 2003

**Abstract**

Since, especially for higher frequencies, Timoshenko's theory gives more reliable results than Euler–Bernoulli's theory, systems of beams, like frames, under arbitrary dynamic excitations should be analyzed on the basis of this refined theory. In this paper, after deriving the basic fundamental solutions of a lateral unit point force and of a unit single moment, the deflection and the rotation of the beam cross-section are given as integral equation forms of the governing second order differential equation system in the Laplace and the frequency domain. Since in frameworks axial displacements also occur, the well-known integral equations for bars under tension or compression are added to complete the modelling of plane frame structures. From these, the unknown boundary values may be exactly determined via point collocation at the beam ends and solution of the resulting algebraic system. With these boundary values, the exact deflection and rotation can also be found at arbitrary interior points. Finally, the convolution quadrature method is applied to the Laplace domain integral equation formulation in order to analyze the time-dependent wave propagation process. Two examples are presented to demonstrate the method's exactness compared with conventional finite element results: a single beam where the shift of the resonance frequencies when using the Timoshenko theory instead of Euler–Bernoulli's theory is shown, and a two-storey framework where, in addition to the frequence response, the causality of the propagating wave is studied.


## 1. Introduction

The importance of shear deformation and rotatory inertia in the description of the dynamic response of beams is well documented [1] and a first improved theory was already given by

*Corresponding author. Institute of Applied Mechanics, University Carolo Wilhelmina, Braunschweig 38023, Germany. Tel.: +49-531-3917-100; fax: +49-531-3915-843.
*E-mail address:* h.antes@tu-bs.de (H. Antes).

0022-460X/$ - see front matter 
doi:10.1016/j.jsv.2003.08.048

Timoshenko in 1921. In time domain, the more exact Timoshenko theory has a hyperbolic character, opposite to the ellipticity of the Euler–Bernoulli theory [2], i.e. the refined theory has wave character [3]. An especially important aspect in dynamic analyses of beams is the prediction of natural frequencies and mode shapes. Studies of several investigators (e.g. [4]) show that the effects of rotatory inertia and shear deformation on the first mode of vibrations are small, but that they increase rapidly for the second and higher modes.

Hence, dependent on the actual bending wave length and on the beam cross sectional dimensions, Timoshenko's theory gives more reliable results than Euler–Bernoulli's theory [5], i.e., Euler–Bernoulli theory is exact enough only for wave lengths $\lambda \geqslant 10r$ in the case of a beam with circular cross-section of radius $r$, or when the ratio of the radius of gyration of the cross-section of the beam to its length is very small, say in the order of $10^{-4}$ [6]. Consequently, for beams and systems of beams like frames under arbitrary dynamic excitations, an analysis should be based on Timoshenko's theory.

Since in structural mechanics the finite element method (FEM) is mostly applied in practice, also for Timoshenko beams several studies are known which present different element types and formulations. The Kapur element [7], for example, is based on a cubic displacement expansion for both the bending (that portion of the transverse displacement that is attributed to flexural deformation) displacement and the shear (that part due to shearing deformations) displacement, while other formulations are written in terms of the transverse beam deflection and normal rotation, derived either from Gurtin's variational principle [8] or from the mixed principles of Reissner and Hu-Washizu [9].

Although not being a conventional, h- or p-version of the FEM, it is important to mention in this context the work of Ovunc [10] and of Beskos et al. [11,12] where the exact solutions of the homogeneous harmonic equations of motions of beams are applied in a dynamic stiffness approach and the mass is assumed to be continuously distributed which provides the exact response. The dynamic response of frameworks to general transient forces can be obtained by applying the dynamic stiffness method in conjunction with either modal analysis [10] or with a numerical inversion of the transformed solution [12]. As stated by the authors [12], there are only two disadvantages with this last method: firstly, it requires more computer time for the numerical Laplace inversion than step-by-step integration schemes, and, secondly, it is not possible to give explicit expressions of the dynamic stiffness coefficients $D_{ij}$ for a Timoshenko beam. In using solutions of the governing homogeneous differential equations as 'shape functions', this methodology is also related to the method of fundamental solutions (MFS) where linear combinations of fundamental solutions are applied to approximate the solution [13] which can be viewed as either an indirect boundary element method or a modified Trefftz method.

In recent years, the direct version of boundary element method (BEM) has been developed for the numerical solution of various engineering mechanic problems as an alternative to the finite element method. For Euler–Bernoulli beams, again Beskos was one of the first to apply the BEM to free and forced flexural vibration problems [14] but not yet for the refined theory of Timoshenko.

Recently, this gap has been filled for the static case [15]. Here, a corresponding study is presented for the more important dynamic analysis where the most difficult problem is the analytic derivation of the necessary fundamental solutions for the dynamic Timoshenko beam problem in the Laplace transform domain and in the frequency domain. Moreover, the related

boundary integral equations are given in their direct form. Since the only known time domain fundamental solution of the fourth order differential equation for the Timoshenko vibration problem (see Ref. [16]) is not easily applicable in the respective integral equations because it is found in a form containing integrals which can only be evaluated numerically, here, the quadrature convolution method [17–19] is applied to determine time-dependent responses to transient dynamic excitations.

Adding the well-known integral equations for the dynamic response of bars under tension, arbitrary plane frame structures can be modelled by adequate combinations of these equations. Some simple examples are presented which show the importance of using the Timoshenko beam theory in dynamic analyses of plane frameworks, especially for high excitation frequencies.

## 2. Governing equations of plane frame dynamics

In plane frameworks, dynamic reactions of beams as well as of bars may be activated dependent on the actual excitation and on the structure's geometry, i.e., flexural waves and longitudinal waves are produced which may dynamically interact with each other. For an analysis of these effects, the equations of motions for beams and bars have to be combined and assembled according to the actual plane structure.

### 2.1. Vibrations of Timoshenko beams

During vibration, the elements of a beam perform not only a translatory motion but also rotate. Hence, when taking into account not only the rotatory inertia but also the deflection due to shear, the slope of the deflection curve $w$ depends not only on the rotation $\varphi$ of the beam cross-section but also on the shear, i.e. on the angle of shear $\gamma_{xz}$ at the neutral axis:

$$\frac{\partial}{\partial x} w(x,t) = -\varphi(x,t) + \gamma_{xz}(x,t). \tag{1}$$

From the elementary Euler–Bernoulli theory of bending one has the following relations for the bending moment $M$ and the shearing force $Q$:

$$M(x,t) = EI \frac{\partial}{\partial x} \varphi(x,t), \tag{2}$$

$$Q(x,t) = \kappa GA\gamma_{xz} = \kappa GA\left(\frac{\partial w(x,t)}{\partial x} + \varphi(x,t)\right) \tag{3}$$

in which $EI$ is the flexural rigidity, $A$ is the cross-sectional area, $G$ is the shear modulus, and $\kappa$, the so-called shear coefficient is a factor which gives the ratio of the average shear strain on a section to the shear strain at the centroid (for details, see Ref. [20]). Its value is dependent on the shape of cross-section, but also, as pointed out by Cowper [21], on the material's Poisson ratio $\nu$, and, moreover, for dynamic problems on the considered frequency range. Hence, different approximations exist, e.g., that of Roark [22] for only static deflections with $\kappa = 0.9$ and $\kappa = 5/6$ for a circular and a rectangular cross-section respectively. For static as well as low-frequency deformations of beams, Cowper [21] gave for these cross-sections the values

$\kappa_{circle} = 6(1+\nu)/(7+6\nu)$ and $\kappa_{rectangle} = 10(1+\nu)/(12+11\nu)$ and, additionally, a rather great listing of shear coefficients for thin-walled cross-sections. For high-frequency vibration modes, one should consider the values of Mindlin and Deresiewicz [23] and of Goodmann [24].

Considering the dynamic equilibrium, i.e., the equation of motion in the vertical $z$ direction gives

$$\frac{\partial}{\partial x} Q(x,t) + q(x,t) = \rho A \frac{\partial^2}{\partial t^2} w(x,t), \tag{4}$$

where $q(x,t)$ is the distributed lateral dynamic load on the beam and $\rho$ is the density of the beam material per unit volume. Then, summing up the moments about the $y$-axis through the centre of a beam element of length $\mathrm{d}x$ yields

$$\frac{\partial}{\partial x} M(x,t) - Q(x,t) + m(x,t) = \rho I \frac{\partial^2}{\partial t^2} \varphi(x,t), \tag{5}$$

where $m(x,t)$ means an action of prescribed distributed moments and $I$ is the moment of inertia about the $y$-axis.

Finally, substituting the constitutive relations (2) and (3) into the two governing differential equations (4) and (5), one obtains the following coupled system in a differential operator notation:

$$\mathbf{B}_t \begin{bmatrix} w \\ \varphi \end{bmatrix} = \begin{bmatrix} \left(\kappa GA \dfrac{\partial^2}{\partial x^2} - \rho A \dfrac{\partial^2}{\partial t^2}\right) & \kappa GA \dfrac{\partial}{\partial x} \\ -\kappa GA \dfrac{\partial}{\partial x} & \left(EI \dfrac{\partial^2}{\partial x^2} - \kappa GA - \rho I \dfrac{\partial^2}{\partial t^2}\right) \end{bmatrix} \begin{bmatrix} w \\ \varphi \end{bmatrix} = - \begin{bmatrix} q \\ m \end{bmatrix}. \tag{6}$$

For harmonic loadings $q(x,t) = \hat{q}(x)\mathrm{e}^{\mathrm{i}\omega t}$ and $m(x,t) = \hat{m}(x)\mathrm{e}^{\mathrm{i}\omega t}$ with the same excitation frequency $\omega$ or only one type of excitation, i.e., either $q(x,t) = 0$ or $m(x,t) = 0$, both responses are also harmonic with this frequency, and their amplitudes $\hat{w}(x)$ and $\hat{\varphi}(x)$ are described by

$$\mathbf{B}_\omega \begin{bmatrix} \hat{w} \\ \hat{\varphi} \end{bmatrix} = \begin{bmatrix} \kappa GA \dfrac{\partial^2}{\partial x^2} + \rho A\omega^2 & \kappa GA \dfrac{\partial}{\partial x} \\ -\kappa GA \dfrac{\partial}{\partial x} & EI \dfrac{\partial^2}{\partial x^2} - \kappa GA + \rho I\omega^2 \end{bmatrix} \begin{bmatrix} \hat{w} \\ \hat{\varphi} \end{bmatrix} = - \begin{bmatrix} \hat{q} \\ \hat{m} \end{bmatrix}. \tag{7}$$

When the two dynamic loadings $q(x,t)$ and $m(x,t)$ are arbitrary or are both harmonic but with different excitation frequencies, and, moreover, since the convolution quadrature method will be applied to determine time-dependent solutions, the Laplace transform technique with respect to time with the general complex transform parameter $s$, i.e.,

$$\hat{f}(x,s) = \mathscr{L}(f(x,t)) = \int_0^\infty \mathrm{e}^{-st} f(x,t)\,\mathrm{d}t \quad \text{with } \mathscr{R}e(s) > 0 \tag{8}$$

has to be applied to all state functions for removing the time dependence. Assuming zero initial conditions, the transformation of the system (6) gives

$$\mathbf{B}_s \begin{bmatrix} \hat{w} \\ \hat{\varphi} \end{bmatrix} = \begin{bmatrix} \left(\kappa GA \dfrac{\partial^2}{\partial x^2} - \rho A s^2\right) & \kappa GA \dfrac{\partial}{\partial x} \\ -\kappa GA \dfrac{\partial}{\partial x} & \left(EI \dfrac{\partial^2}{\partial x^2} - \kappa GA - \rho I s^2\right) \end{bmatrix} \begin{bmatrix} \hat{w} \\ \hat{\varphi} \end{bmatrix} = - \begin{bmatrix} \bar{q}(x,s) \\ \bar{m}(x,s) \end{bmatrix}. \tag{9}$$

As is well-known, the two coupled differential equations of the second order (6) can be transformed into one differential equation of the fourth order by eliminating the state $\varphi$ where the main part, i.e., the fourth order terms can be written as a product of two wave equation operators as

$$\left(\frac{\partial^2}{\partial t^2}-c_2^2\frac{\partial^2}{\partial x^2}\right)\left(\frac{\partial^2}{\partial t^2}-c_1^2\frac{\partial^2}{\partial x^2}\right)w+\frac{A}{I}c_2^2\frac{\partial^2 w}{\partial t^2}=\frac{c_2^2}{\rho I}\left(q+\frac{\partial m}{\partial x}\right)-\frac{1}{\rho A}\left(c_1^2\frac{\partial^2 q}{\partial x^2}-\frac{\partial^2 q}{\partial t^2}\right), \tag{10}$$

with the propagation velocities $c_1=\sqrt{E/\rho}$ and $c_2=\sqrt{\kappa G/\rho}$ of the longitudinal wave and the shear wave respectively.

### 2.2. Longitudinal waves in elastic beams

The dynamic equilibrium of a bar element with the cross-section $A$ and material density $\rho$ under an axial loading $\bar{n}(x,t)$ and a longitudinal acceleration $\ddot{u}(x)=\partial^2 u(x,t)/\partial t^2$ is described by

$$\frac{\partial N(x,t)}{\partial x}=-\bar{n}(x,t)+\rho A\frac{\partial^2 u(x,t)}{\partial t^2}, \tag{11}$$

where the axial resultant force $N(x,t)$ is related to the longitudinal displacement $u(x,t)$ by

$$N(x,t)=EA\frac{\partial u(x,t)}{\partial x}=EAu'(x,t). \tag{12}$$

Connecting both equations and assuming constant cross-section $A$ and modulus of elasticity $E$ yields the basic differential equation

$$EA\frac{\partial^2 u(x,t)}{\partial x^2}=-\bar{n}(x,t)+\rho A\frac{\partial^2 u(x,t)}{\partial t^2}, \tag{13}$$

or, introducing the longitudinal wave speed $c_L=\sqrt{E/\rho}$,

$$\frac{\partial^2 u(x,t)}{\partial x^2}-\frac{1}{c_L^2}\frac{\partial^2 u(x,t)}{\partial t^2}=-\frac{\bar{n}(x,t)}{EA}. \tag{14}$$

For time-harmonic loadings with the excitation frequency $\omega$, the response can also be assumed to be time-harmonic i.e.:

$$\bar{n}(x,t)=\hat{n}(x)e^{i\omega t}\rightarrow u(x,t)=\hat{u}(x)e^{i\omega t}. \tag{15}$$

The result is an equation which is no longer time-dependent and is of the Helmholtz type

$$\frac{d^2\hat{u}(x)}{dx^2}+k^2\hat{u}(x)=-\frac{\hat{n}(x)}{EA}. \tag{16}$$

The ratio $k=\omega/c_L$ is the so-called wave number.

Applying the Laplace transform technique with respect to time (see Eq. (8)) to all state functions and assuming zero initial conditions, the transformed equation (13) reads as

$$\left[EA\frac{\partial^2}{\partial x^2}-\rho As^2\right][\hat{u}(x,s)]=-\hat{n}(x,s), \tag{17}$$

or corresponding to Eq. (14) as

$$\frac{\partial^2 \hat{u}(x,s)}{\partial x^2} - \frac{s^2}{c_L^2}\hat{u}(x,s) = -\frac{\hat{n}(x,s)}{EA}. \tag{18}$$

## 3. Fundamental solutions

Dependent on the actual problem, the dynamic analysis of beams is performed either in the time domain, e.g., when transient excitations act on the system, or in the frequency domain, e.g., when the excitations are harmonic.

In the time domain, the only fundamental solution for beams which is, to the authors knowledge, known for Timoshenko beam equations, is that of the most difficult one, of the fourth order time-dependent equation (10) in the papers of Ortner and Wagner [16,25]. But, this fundamental solution contains complicated integrals which can be evaluated only numerically by quadrature formula, and is, maybe due to this fact, rarely applied.

To avoid the time dependence in the case of arbitrary dynamic excitations, the fundamental solutions of the Laplace domain formulation (9) for the Timoshenko beam and of (17) for the bar are of interest. It should be mentioned that, in the following, the dependence of all state functions from the Laplace parameter $s$ is omitted in order to shorten the expressions.

### 3.1. Timoshenko beam solutions

In Timoshenko's beam theory, the sought fundamental solutions are the responses of an infinite beam to a unit impulsive point force $\hat{q}^*(x) = \delta(x-\xi)$ and to a unit impulsive moment $\hat{m}^*(x) = \delta(x-\xi)$, respectively, at the point $\xi$.

#### 3.1.1. In the Laplace domain

In a short operator notation, the fundamental solution matrix $\mathbf{G}$ is defined by ($r = |x-\xi|$)

$$\begin{aligned}\mathbf{B}_s\mathbf{G} &= \begin{bmatrix} \left(D_1\dfrac{\partial^2}{\partial x^2} - S_1\right) & D_1\dfrac{\partial}{\partial x} \\ -D_1\dfrac{\partial}{\partial x} & \left(D_2\dfrac{\partial^2}{\partial x^2} - D_1 - S_2\right) \end{bmatrix} \begin{bmatrix} \hat{w}_q^\infty(x,\xi) & \hat{w}_m^\infty(x,\xi) \\ \hat{\varphi}_q^\infty(x,\xi) & \hat{\varphi}_m^\infty(x,\xi) \end{bmatrix} \\ &= -\mathbf{I}\delta(x-\xi) = -\begin{bmatrix} \delta(x-\xi) & 0 \\ 0 & \delta(x-\xi) \end{bmatrix}, \end{aligned} \tag{19}$$

with $D_1 = \kappa GA$, $D_2 = EI$, $S_1 = \rho A s^2$, and $S_2 = \rho I s^2$ (see, definition (9)). Then, following the ideas of Hörmander [26], the fundamental solutions are found from a scalar function $\psi$ via the matrix of cofactors $(\mathbf{B}_s)^{co}$ of $\mathbf{B}_s$:

$$\mathbf{G} = (\mathbf{B}_s)^{co}\psi = \begin{bmatrix} \left(D_2\dfrac{\partial^2}{\partial x^2} - D_1 - S_2\right) & -D_1\dfrac{\partial}{\partial x} \\ D_1\dfrac{\partial}{\partial x} & \left(D_1\dfrac{\partial^2}{\partial x^2} - S_1\right) \end{bmatrix}\psi, \tag{20}$$

since one has, due to

$$\mathbf{B}_s(\mathbf{B}_s)^{-1} = \mathbf{I} \quad \text{with } (\mathbf{B}_s)^{-1} = \frac{(\mathbf{B}_s)^{co}}{\det(\mathbf{B}_s)}, \tag{21}$$

from

$$\mathbf{B}_s\mathbf{G} = \mathbf{B}_s(\mathbf{B}_s)^{co}\psi = \det(\mathbf{B}_s)\mathbf{I}\psi = -\mathbf{I}\delta(x-\xi), \tag{22}$$

the defining equation

$$\det(\mathbf{B}_s)\psi = -\delta(x-\xi). \tag{23}$$

Hence, the method of finding the fundamental solutions is reduced to determining the scalar function $\psi$. The matrix of the fundamental solutions is then found via Eq. (20), i.e., by applying the matrix of cofactors $(\mathbf{B}_s)^{co}$ on $\psi$.

Since here the determinant of the operator matrix $\mathbf{B}_s$ is

$$\begin{aligned}\det(\mathbf{B}_s) &= \left(D_1\frac{\partial^2}{\partial x^2} - S_1\right)\left(D_2\frac{\partial^2}{\partial x^2} - D_1 - S_2\right) - D_1\frac{\partial}{\partial x}\left(-D_1\frac{\partial}{\partial x}\right)\\ &= D_1D_2\frac{\partial^4}{\partial x^4} - (D_1S_2 + D_2S_1)\frac{\partial^2}{\partial x^2} + S_1(D_1+S_2),\end{aligned} \tag{24}$$

the two roots of $\det(\mathbf{B}_s) = 0$ are

$$\begin{aligned}\lambda_{1,2} &= \frac{1}{2D_1D_2}\left[(D_1S_2 + D_2S_1) \pm \sqrt{(D_1S_2 + D_2S_1)^2 - 4D_1D_2S_1(D_1+S_2)}\right]\\ &= \frac{1}{2}\left[\left(\frac{\rho s^2}{E} + \frac{\rho s^2}{\kappa G}\right) \pm \sqrt{\left(\frac{\rho s^2}{E} - \frac{\rho s^2}{\kappa G}\right)^2 - 4\frac{\rho A s^2}{EI}}\right]\\ &= \frac{s^2}{2}\left[\left(\frac{1}{c_1^2} + \frac{1}{c_2^2}\right) \pm \frac{1}{c_1^2}\sqrt{\left(1 - \frac{c_1^2}{c_2^2}\right)^2 - \frac{4c_1^2A}{s^2I}}\right],\end{aligned} \tag{25}$$

and Eq. (23) can be represented with these roots as

$$\left(\frac{\partial^4}{\partial x^4} - (\lambda_1+\lambda_2)\frac{\partial^2}{\partial x^2} + \lambda_1\lambda_2\right)\psi = \left(\frac{\partial^2}{\partial x^2} - \lambda_1\right)\left(\frac{\partial^2}{\partial x^2} - \lambda_2\right)\psi = -\frac{\delta(x-\xi)}{D_1D_2}. \tag{26}$$

From several publications, e.g., from Cheng and Antes [27], one knows its solution

$$\psi = \frac{1}{2D_1D_2(\lambda_1-\lambda_2)}\left[\frac{e^{-\sqrt{\lambda_1}r}}{\sqrt{\lambda_1}} - \frac{e^{-\sqrt{\lambda_2}r}}{\sqrt{\lambda_2}}\right], \tag{27}$$

and finds via Eq. (20) the fundamental solution due to a unit force impulse at $x=\xi$ ($r_{,x}=2H(x-\xi)-1$):

$$\hat{w}_q^*(x,\xi)=\left(D_2\frac{\partial^2}{\partial x^2}-D_1-S_2\right)\psi$$
$$=\frac{1}{2D_1(\lambda_1-\lambda_2)}\left[\frac{\mathrm{e}^{-\sqrt{\lambda_1}r}}{\sqrt{\lambda_1}}\left(\lambda_1-\frac{D_1+S_2}{D_2}\right)-\frac{\mathrm{e}^{-\sqrt{\lambda_2}r}}{\sqrt{\lambda_2}}\left(\lambda_2-\frac{D_1+S_2}{D_2}\right)\right] \tag{28}$$

$$\hat{\varphi}_q^*(x,\xi)=D_1\frac{\partial}{\partial x}\psi=\frac{-r_{,x}}{2D_2(\lambda_1-\lambda_2)}\left[\mathrm{e}^{-\sqrt{\lambda_1}r}-\mathrm{e}^{-\sqrt{\lambda_2}r}\right], \tag{29}$$

and also that due to a unit impulsive moment at $x=\xi$

$$\hat{w}_m^*(x,\xi)=-D_1\frac{\partial}{\partial x}\psi=-\hat{\varphi}_q^*(x,\xi)=\frac{r_{,x}}{2D_2(\lambda_1-\lambda_2)}\left[\mathrm{e}^{-\sqrt{\lambda_1}r}-\mathrm{e}^{-\sqrt{\lambda_2}r}\right], \tag{30}$$

$$\hat{\varphi}_m^*(x,\xi)=\left(D_1\frac{\partial^2}{\partial x^2}-S_1\right)\psi$$
$$=\frac{1}{2D_2(\lambda_1-\lambda_2)}\left[\frac{\mathrm{e}^{-\sqrt{\lambda_1}r}}{\sqrt{\lambda_1}}\left(\lambda_1-\frac{S_1}{D_1}\right)-\frac{\mathrm{e}^{-\sqrt{\lambda_2}r}}{\sqrt{\lambda_2}}\left(\lambda_2-\frac{S_1}{D_1}\right)\right]. \tag{31}$$

Although this fact is only important for beams of infinite length, it should be mentioned that these Laplace domain fundamental solutions (28)–(31) satisfy the so-called Sommerfeld radiation condition, i.e., they tend with $\mathscr{R}e(\lambda_1)>0$ and $\mathscr{R}e(\lambda_2)>0$ to zero for $r\to 0$.

*3.1.2. In the frequency domain*

In the harmonic case, i.e., for excitations with a frequency $\omega$, the adequate defining equation (23) is obtained by $s=\mathrm{i}\omega$, ($\mathrm{i}^2=-1$), and $S_1=-\rho A\omega^2$ as well as $S_2=-\rho I\omega^2$ in Eq. (24). Then, both these roots (25) are real-valued with $c_1^2=E/\rho$ and $c_2^2=\kappa G/\rho$:

$$\lambda_{1,2}=-\frac{\omega^2}{2}\left[\left(\frac{1}{c_1^2}+\frac{1}{c_2^2}\right)\pm\frac{1}{c_1^2}\sqrt{\left(1-\frac{c_1^2}{c_2^2}\right)^2+4\frac{c_1^2A}{\omega^2I}}\right], \tag{32}$$

and, obviously, $\lambda_1<0$ holds for all $\omega$, while, as one can easily find, $\lambda_2<0$ for $\omega^2>\kappa GA/\rho I$ and $\lambda_2>0$ for $\omega^2<\kappa GA/\rho I$. Consequently, since the corresponding fundamental solutions should also be real-valued, one has to consider two solutions of Eq. (26):

$$\psi=\frac{1}{2D_1D_2(\lambda_2-\lambda_1)}\left[\frac{\sin\left(\sqrt{-\lambda_1}r\right)}{\sqrt{-\lambda_1}}-\frac{\sin\left(\sqrt{-\lambda_2}r\right)}{\sqrt{-\lambda_2}}\right]\quad\text{for }\lambda_1<\lambda_2<0, \tag{33}$$

$$\psi=\frac{1}{2D_1D_2(\lambda_2-\lambda_1)}\left[\frac{\sin\left(\sqrt{-\lambda_1}r\right)}{\sqrt{-\lambda_1}}+\frac{\mathrm{e}^{-\sqrt{\lambda_2}r}}{\sqrt{\lambda_2}}\right]\quad\text{for }\lambda_1<0<\lambda_2. \tag{34}$$

Hence, one has two sets of fundamental solutions, i.e., for $\lambda_1<\lambda_2<0$:

$$\hat{w}_q^*(x,\xi)=\frac{1}{2D_1(\lambda_2-\lambda_1)}\left[\frac{\sin\left(\sqrt{-\lambda_2}r\right)}{\sqrt{-\lambda_2}}\left(\frac{D_1+S_2}{D_2}-\lambda_2\right)-\frac{\sin\left(\sqrt{-\lambda_1}r\right)}{\sqrt{-\lambda_1}}\left(\frac{D_1+S_2}{D_2}-\lambda_1\right)\right], \quad (35)$$

$$\hat{\varphi}_q^*(x,\xi)=\frac{r_{,x}}{2D_2(\lambda_2-\lambda_1)}\left[\cos\left(\sqrt{-\lambda_1}r\right)-\cos\left(\sqrt{-\lambda_2}r\right)\right], \quad (36)$$

$$\hat{w}_m^*(x,\xi)=-\hat{\varphi}_q^{\infty}(x,\xi)=\frac{-r_{,x}}{2D_2(\lambda_2-\lambda_1)}\left[\cos\left(\sqrt{-\lambda_1}r\right)-\cos\left(\sqrt{-\lambda_2}r\right)\right], \quad (37)$$

$$\hat{\varphi}_m^*(x,\xi)=\frac{1}{2D_2(\lambda_2-\lambda_1)}\left[\frac{\sin\left(\sqrt{-\lambda_2}r\right)}{\sqrt{-\lambda_2}}\left(\frac{S_1}{D_1}-\lambda_2\right)-\frac{\sin\left(\sqrt{-\lambda_1}r\right)}{\sqrt{-\lambda_1}}\left(\frac{S_1}{D_1}-\lambda_1\right)\right]; \quad (38)$$

for $\lambda_1<0<\lambda_2$ :

$$\hat{w}_q^*(x,\xi)=\frac{-1}{2D_1(\lambda_2-\lambda_1)}\left[\frac{e^{-\sqrt{\lambda_2}r}}{\sqrt{\lambda_2}}\left(\frac{D_1+S_2}{D_2}-\lambda_2\right)+\frac{\sin\left(\sqrt{-\lambda_1}r\right)}{\sqrt{-\lambda_1}}\left(\frac{D_1+S_2}{D_2}-\lambda_1\right)\right], \quad (39)$$

$$\hat{\varphi}_q^*(x,\xi)=\frac{r_{,x}}{2D_2(\lambda_2-\lambda_1)}\left[\cos\left(\sqrt{-\lambda_1}r\right)-e^{-\sqrt{\lambda_2}r}\right], \quad (40)$$

$$\hat{w}_m^*(x,\xi)=-\hat{\varphi}_q^{\infty}(x,\xi)=\frac{-r_{,x}}{2D_2(\lambda_2-\lambda_1)}\left[\cos\left(\sqrt{-\lambda_1}r\right)-e^{-\sqrt{\lambda_2}r}\right], \quad (41)$$

$$\hat{\varphi}_m^*(x,\xi)=\frac{-1}{2D_2(\lambda_2-\lambda_1)}\left[\frac{e^{-\sqrt{\lambda_2}r}}{\sqrt{\lambda_2}}\left(\frac{S_1}{D_1}-\lambda_2\right)+\frac{\sin\left(\sqrt{-\lambda_1}r\right)}{\sqrt{-\lambda_1}}\left(\frac{S_1}{D_1}-\lambda_1\right)\right]. \quad (42)$$

### 3.2. Bar solutions

In the frequency domain, the adequate fundamental solution of the Helmholtz equation (16), i.e., the axial displacement response of an infinite bar to a unit harmonic axial point forces $\hat{n}(x)=\delta(x-\xi)$ acting at point $\xi$, is well known to be ($k=\omega/c_L$)

$$u^*(x,\xi)=\frac{-1}{2kEA}\sin(kr). \quad (43)$$

Its correctness can easily be demonstrated, since its first and second derivative, respectively, is

$$\frac{\partial u^*(x,\xi)}{\partial x}=\frac{-1}{2EA}\cos(kr)\frac{\partial r}{\partial x}=\frac{-1}{2EA}\cos(kr)[2H(x-\xi)-1], \quad (44)$$

$$\frac{\partial^2 u^*(x,\xi)}{\partial x^2}=\frac{k}{2EA}\sin(kr)-\frac{\cos(kr)}{EA}\delta(x-\xi), \quad (45)$$

such that

$$\int_0^l \left[\frac{\partial^2 u^*(x,\xi)}{\partial x^2} + k^2 u^*(x,\xi)\right] u(x)\,\mathrm{d}x = -\int_0^l \frac{\cos(kr)}{EA}\,\delta(x-\xi)u(x)\,\mathrm{d}x = \frac{-u(\xi)}{EA} \quad \text{for } \xi \in [0,l]. \tag{46}$$

In the Laplace domain, the basic differential equation (18)

$$\frac{\partial^2}{\partial x^2}\hat{u}(x,s) - h^2\hat{u}(x,s) = -\frac{\hat{n}(x,s)}{EA}, \tag{47}$$

with $h = s/c_L$ is also of the Helmholtz type, but has a minus sign in front of the complex $h^2$ factor. Hence, the respective fundamental solution, i.e., the solution for $\hat{n}(x,s) = \delta(x-\xi)$ is either

$$u^*(x,\xi) = \frac{1}{2hEA}\,\mathrm{e}^{-hr}, \tag{48}$$

or

$$u^*(x,\xi) = \frac{-1}{2hEA}\sinh(hr), \tag{49}$$

which can easily be checked following the above steps (44)–(46).

### 3.3. Transition to the static case

Since the differential equations (7) and (9) for the dynamic problem give directly with $\omega = 0$ and $s = 0$, respectively, the corresponding static system

$$\mathbf{B}_0\begin{bmatrix} w \\ \varphi \end{bmatrix} = \begin{bmatrix} D_1\dfrac{\partial^2}{\partial x^2} & D_1\dfrac{\partial}{\partial x} \\ -D_1\dfrac{\partial}{\partial x} & \left(D_2\dfrac{\partial^2}{\partial x^2} - D_1\right) \end{bmatrix}\begin{bmatrix} w \\ \varphi \end{bmatrix} = -\begin{bmatrix} q \\ m \end{bmatrix}, \tag{50}$$

one would expect also that the dynamic fundamental solutions (28)–(31) of (9) will tend for $\omega \to 0$ or $s \to 0$ to the static fundamental solutions (for details, see Ref. [15])

$$\hat{w}_q^*(x,\xi) = \frac{1}{12D_2}\left[r^3 - 6\frac{D_2}{D_1}r\right], \quad \hat{\varphi}_q^*(x,\xi) = -\frac{r^2}{4D_2}[2H(x-\xi)-1], \tag{51}$$

$$\hat{w}_m^*(x,\xi) = \frac{r^2}{4D_2}[2H(x-\xi)-1], \quad \hat{\varphi}_m^*(x,\xi) = -\frac{r}{2D_2}. \tag{52}$$

#### 3.3.1. Laplace domain solution

Studying the behaviour of the dynamic fundamental solutions by using the series expansion of $\mathrm{e}^{-\sqrt{\lambda}r}$ shows that this is not the case, but it is easy to detect that it is satisfied when taking instead of Eq. (27)

$$\psi = \frac{1}{4D_1D_2}\frac{1}{(\lambda_1-\lambda_2)}\left[\frac{\mathrm{e}^{-\sqrt{\lambda_1}r} - \mathrm{e}^{\sqrt{\lambda_1}r}}{\sqrt{\lambda_1}} - \frac{\mathrm{e}^{-\sqrt{\lambda_2}r} - \mathrm{e}^{\sqrt{\lambda_2}r}}{\sqrt{\lambda_2}}\right]$$

$$= \frac{1}{2D_1D_2}\frac{1}{(\lambda_2-\lambda_1)}\left[\frac{\sinh\left(\sqrt{\lambda_1}r\right)}{\sqrt{\lambda_1}} - \frac{\sinh\left(\sqrt{\lambda_2}r\right)}{\sqrt{\lambda_2}}\right], \tag{53}$$

i.e., adding $e^{\sqrt{\lambda_1}r}$ and $e^{\sqrt{\lambda_2}r}$, respectively, gives a scalar function $\psi$ whose series expansion tends to the static case, i.e., $\psi = -r^3/12D_1D_2$. Hence, the fundamental solutions derived from Eq. (53)

$$\hat{w}_q^*(x,\xi) = \frac{1}{2D_1}\frac{1}{(\lambda_2-\lambda_1)}\left[\frac{\sinh\left(\sqrt{\lambda_1}r\right)}{\sqrt{\lambda_1}}\left(\lambda_1 - \frac{D_1+S_2}{D_2}\right) - \frac{\sinh\left(\sqrt{\lambda_2}r\right)}{\sqrt{\lambda_2}}\left(\lambda_2 - \frac{D_1+S_2}{D_2}\right)\right], \tag{54}$$

$$\hat{\varphi}_q^*(x,\xi) = \frac{1}{2D_2}\frac{r_{,x}}{(\lambda_2-\lambda_1)}\left[\cosh\left(\sqrt{\lambda_1}r\right) - \cosh\left(\sqrt{\lambda_2}r\right)\right] = -\hat{w}_m^*(x,\xi), \tag{55}$$

$$\hat{\varphi}_m^*(x,\xi) = \frac{1}{2D_2}\frac{1}{(\lambda_2-\lambda_1)}\left[\frac{\sinh\left(\sqrt{\lambda_1}r\right)}{\sqrt{\lambda_1}}\left(\lambda_1 - \frac{S_1}{D_1}\right) - \frac{\sinh\left(\sqrt{\lambda_2}r\right)}{\sqrt{\lambda_2}}\left(\lambda_2 - \frac{S_1}{D_1}\right)\right], \tag{56}$$

contain, as a special case with $s\to 0$, the static problem, but they no longer satisfy the Sommerfeld radiation condition.

### 3.3.2. Frequency domain solution

For the harmonic excitation cases, i.e., for Eqs. (33) and (34), one can easily find that for the case with $\lambda_1<\lambda_2<0$ the function $\psi$ in the form (33) tends for $\omega\to 0$, i.e., $\lambda_1\to 0$ and $\lambda_2\to 0$, to the respective static function $\psi = -r^3/12D_1D_2$. This is not the case for Eq. (34), i.e., for $\lambda_1<0<\lambda_2$: there one should use

$$\psi = \frac{1}{2D_1D_2(\lambda_2-\lambda_1)}\left[\frac{\sin\left(\sqrt{-\lambda_1}r\right)}{\sqrt{-\lambda_1}} - \frac{\sinh\left(\sqrt{\lambda_2}r\right)}{\sqrt{\lambda_2}}\right].$$

This case is only relevant if small frequencies $\omega$ are considered since $\lambda_2>0$ for $\omega^2<\kappa GA/\rho I$. Hence, for such cases the following fundamental solutions should be applied:

$$\hat{w}_q^*(x,\xi) = \frac{1}{2D_1(\lambda_2-\lambda_1)}\left[\frac{\sin\left(\sqrt{-\lambda_1}r\right)}{\sqrt{-\lambda_1}}\left(\lambda_1 - \frac{D_1+S_2}{D_2}\right) - \frac{\sinh\left(\sqrt{\lambda_2}r\right)}{\sqrt{\lambda_2}}\left(\lambda_2 - \frac{D_1+S_2}{D_2}\right)\right], \tag{57}$$

$$\hat{\varphi}_q^*(x,\xi) = \frac{r_{,x}}{2D_2(\lambda_2-\lambda_1)}\left[\cos\left(\sqrt{-\lambda_1}r\right) - \cosh\left(\sqrt{\lambda_2}r\right)\right] = -\hat{w}_m^*(x,\xi), \tag{58}$$

$$\hat{\varphi}_m^*(x,\xi) = \frac{1}{2D_2(\lambda_2-\lambda_1)}\left[\frac{\sin\left(\sqrt{-\lambda_1}r\right)}{\sqrt{-\lambda_1}}\left(\lambda_1 - \frac{S_1}{D_1}\right) - \frac{\sinh\left(\sqrt{\lambda_2}r\right)}{\sqrt{\lambda_2}}\left(\lambda_2 - \frac{S_1}{D_1}\right)\right]. \tag{59}$$

Both the fundamental solutions (43) and (49) of the dynamic bar problem in the frequency domain and the Laplace domain, respectively, tend for $\omega\to 0$ and $s\to 0$, respectively, to the static fundamental solution $u^\infty(x,\xi) = -r/2EA$ , whereas the fundamental solution (48) satisfies the Sommerfeld radiation condition, but not the transition to the static case.

## 4. Integral equation formulations

The most general methodology of deriving equivalent integral equations from differential equations is the method of weighted residuals, since it is applicable without other specific information such as reciprocal theorems.

### 4.1. Timoshenko beam integral equations

For equation system (9), the starting equation is its residual weighted by the matrix **G** of the relevant fundamental solutions (28)–(31), i.e., it holds for $\xi \in [0, l]$

$$\int_0^l \left( \mathbf{B}_s \begin{bmatrix} \hat{w}(x) \\ \hat{\varphi}_y(x) \end{bmatrix} + \begin{bmatrix} \hat{q}(x) \\ \hat{m}(x) \end{bmatrix} \right)^{\mathrm{T}} \begin{bmatrix} \hat{w}_q^*(x,\xi) & \hat{w}_m^*(x,\xi) \\ \hat{\varphi}_q^*(x,\xi) & \hat{\varphi}_m^*(x,\xi) \end{bmatrix} \mathrm{d}x = 0. \tag{60}$$

This gives explicitly the two equations ($\hat{w}' = \partial \hat{w}/\partial x$ a.s.o.)

$$\int_0^l \left\{ \begin{array}{l} [D_1 \hat{w}'' - S_1 \hat{w} + D_1 \hat{\varphi}'] \hat{w}_q^* \\ \quad + [-D_1 \hat{w}' + D_2 \hat{\varphi}'' - (D_1 + S_2)\hat{\varphi}] \hat{\varphi}_q^* \end{array} \right\} \mathrm{d}x = - \int_0^l \begin{bmatrix} \hat{q} \\ \hat{m} \end{bmatrix}^{\mathrm{T}} \begin{bmatrix} \hat{w}_q^* \\ \hat{\varphi}_q^* \end{bmatrix} \mathrm{d}x, \tag{61}$$

$$\int_0^l \left\{ \begin{array}{l} [D_1 \hat{w}'' - S_1 \hat{w} + D_1 \hat{\varphi}'] \hat{w}_m^* \\ \quad + [-D_1 \hat{w}' + D_2 \hat{\varphi}'' - (D_1 + S_2)\hat{\varphi}] \hat{\varphi}_m^* \end{array} \right\} \mathrm{d}x = - \int_0^l \begin{bmatrix} \hat{q} \\ \hat{m} \end{bmatrix}^{\mathrm{T}} \begin{bmatrix} \hat{w}_m^* \\ \hat{\varphi}_m^* \end{bmatrix} \mathrm{d}x, \tag{62}$$

which are formally identical apart from the different weighting fundamental solutions. Now, shifting all differentiations through integrations by parts on the weighting functions yields with the definitions (2) and (3)

$$\begin{aligned} &[\hat{Q}\hat{w}_q^* - \hat{Q}_q^* \hat{w} + \hat{M}\hat{\varphi}_q^* - \hat{M}^* \hat{\varphi}_y]_{x=0}^{x=l} \\ &\quad + \int_0^l \left\{ \begin{array}{l} [D_1 \hat{w}_q^{*\prime\prime} - S_1 \hat{w}_q^* + D_1 \hat{\varphi}_q^{*\prime}] \hat{w} \\ \quad + [D_2 \hat{\varphi}_q^{*\prime\prime} - (D_1 + S_2)\hat{\varphi}_q^* - D_1 \hat{w}_q^{*\prime}] \hat{\varphi}_y \end{array} \right\} \mathrm{d}x = - \int_0^l \left( \begin{array}{l} \hat{q}\hat{w}_q^* \\ \quad + \hat{m}\hat{\varphi}_q^* \end{array} \right) \mathrm{d}x, \end{aligned} \tag{63}$$

and correspondingly

$$\begin{aligned} &[\hat{Q}\hat{w}_m^* - \hat{Q}_m^* \hat{w} + \hat{M}\hat{\varphi}_m^* - \hat{M}_m^* \hat{\varphi}]_{x=0}^{x=l} \\ &\quad + \int_0^l \left\{ \begin{array}{l} [D_1 \hat{w}_m^{*\prime\prime} - S_1 \hat{w}_m^* + D_1 \hat{\varphi}_m^{*\prime}] \hat{w} \\ \quad + [D_2 \hat{\varphi}_m^{*\prime\prime} - (D_1 + S_2)\hat{\varphi}_m^* - D_1 \hat{w}_m^{*\prime}] \hat{\varphi} \end{array} \right\} \mathrm{d}x = - \int_0^l \left( \begin{array}{l} \hat{q}\hat{w}_m^* \\ \quad + \hat{m}\hat{\varphi}_m^* \end{array} \right) \mathrm{d}x. \end{aligned} \tag{64}$$

Finally, by Eq. (19), i.e., taking the filtering effect of the Dirac $\delta(x - \xi)$ into account, one obtains

$$\begin{aligned} \begin{bmatrix} \hat{w}(\xi) \\ \hat{\varphi}(\xi) \end{bmatrix} &= \int_0^l \begin{bmatrix} \hat{w}_q^*(x,\xi) & \hat{w}_m^*(x,\xi) \\ \hat{\varphi}_q^*(x,\xi) & \hat{\varphi}_m^*(x,\xi) \end{bmatrix}^{\mathrm{T}} \begin{bmatrix} \hat{q}(x) \\ \hat{m}(x) \end{bmatrix} \mathrm{d}x \\ &\quad + \left[ \begin{bmatrix} \hat{w}_q^*(x,\xi) & \hat{w}_m^*(x,\xi) \\ \hat{\varphi}_q^*(x,\xi) & \hat{\varphi}_m^*(x,\xi) \end{bmatrix}^{\mathrm{T}} \begin{bmatrix} \hat{Q}(x) \\ \hat{M}(x) \end{bmatrix} - \begin{bmatrix} \hat{Q}_q^*(x,\xi) & \hat{Q}_m^*(x,\xi) \\ \hat{M}_q^*(x,\xi) & \hat{M}_m^*(x,\xi) \end{bmatrix}^{\mathrm{T}} \begin{bmatrix} \hat{w}(x) \\ \hat{\varphi}(x) \end{bmatrix} \right]_{x=0}^{x=l}. \end{aligned} \tag{65}$$

In dynamic frame analyses, the aspect of wave radiation to infinity is not as important as the possibility to also analyze nearly static problems, i.e., problems with very small excitation frequencies. Hence, in the Laplace domain, the fundamental solutions (54)–(56) should be applied, while for small excitation frequencies ($\omega^2 < \kappa GA/\rho I$) in the frequency domain the respective solutions are (57)–(59). The corresponding shear force and bending moment terms may be found in Appendix A.

### 4.2. Bar integral equations

The transformation of the Laplace domain differential equation (47) to an equivalent integral equation may be performed by two integrations by parts of the weighted residual integral over the bar length $l$:

$$\int_0^l \left[\frac{\mathrm{d}^2\hat{u}(x)}{\mathrm{d}x^2} - h^2\hat{u}(x) + \frac{\hat{n}(x)}{EA}\right] u^*(x,\xi)\,\mathrm{d}x = 0, \tag{66}$$

where either the fundamental solution (48) or (49) of the differential equation with $h = s/c_L$ and $c_L = \sqrt{E/\rho}$ is taken as special weighting function. The result

$$\left[\hat{u}'(x)u^*(x,\xi) - \hat{u}(x)\frac{\partial u^*(x,\xi)}{\partial x}\right]_0^l + \int_0^l \left[\frac{\partial^2 u^*(x,\xi)}{\partial x^2} - h^2 u^*(x,\xi)\right]\hat{u}(x)\,\mathrm{d}x = -\int_0^l \frac{\hat{n}(x)}{EA}\,u^*(x,\xi)\,\mathrm{d}x, \tag{67}$$

delivers, when taking the filtering effect of the Dirac function $\delta(x-\xi)$ into account, the following integral expression for the axial displacement at an arbitrary point $\xi \in [0, l]$:

$$\begin{aligned}\hat{u}(\xi) &= \left[EA\hat{u}'(x)u^*(x,\xi) - \hat{u}(x)EA\frac{\partial u^*(x,\xi)}{\partial x}\right]_{x=0}^{x=l} + \int_0^l \hat{n}(x)u^*(x,\xi)\,\mathrm{d}x \\ &= [\hat{N}(x)u^*(x,\xi) - \hat{u}(x)N^*(x,\xi)]_{x=0}^{x=l} + \int_0^l \hat{n}(x)u^*(x,\xi)\,\mathrm{d}x,\end{aligned} \tag{68}$$

where the second boundary state, the axial force $\hat{N}(x)$ was introduced by Eq. (12). The corresponding state of the fundamental solutions (48) or (49) is

$$N^*(x,\xi) = \frac{-r_{,x}}{2}\,\mathrm{e}^{-hr} \quad \text{or} \quad N^*(x,\xi) = \frac{-r_{,x}}{2}\cosh(hr). \tag{69}$$

The integral equation in the frequency domain is formally identical to Eq. (68), only the fundamental solution (48) or (49) and the related axial resultant force (69) have to be substituted by

$$u^*(x,\xi) = \frac{-1}{2kEA}\sin(kr), \quad N^*(x,\xi) = \frac{-r_{,x}}{2}\cos(kr) \quad \text{with } k = \omega/c_L. \tag{70}$$

### 4.3. Boundary (element) equations by collocation

In beam problems, two of the state variables ($\hat{w}, \hat{\varphi}, \hat{Q}, \hat{M}$) at each boundary point, i.e., at $x = 0$ and $x = l$, are always unknown, while in a bar problem only one of the state variables ($\hat{u}, \hat{N}$) has to be determined. Hence, in plane framework problems being, in general, a combination of both, three of the six state variables ($\hat{u}, \hat{w}, \hat{\varphi}, \hat{N}, \hat{Q}, \hat{M}$) are unknown at each of the two boundary points

and, consequently, one needs also three boundary equations at these two boundary points. The simplest way is to evaluate the above systems (65) and (68) at these two points, i.e., to perform point collocation at $\xi = 0 + \varepsilon$ and $\xi = l - \varepsilon$ with $\varepsilon \to 0$:

$$\begin{bmatrix} \mathbf{I} - \mathbf{K}(0,0) & \mathbf{F}(0,0) & \mathbf{K}(l,0) & -\mathbf{F}(l,0) \\ -\mathbf{K}(0,l) & \mathbf{F}(0,l) & \mathbf{I} + \mathbf{K}(l,l) & -\mathbf{F}(l,l) \end{bmatrix} \begin{bmatrix} \mathbf{u}(0) \\ \mathbf{T}(0) \\ \mathbf{u}(l) \\ \mathbf{T}(l) \end{bmatrix} = \int_0^l \begin{bmatrix} \mathbf{F}(x,0) \\ \mathbf{F}(x,l) \end{bmatrix} \begin{bmatrix} \hat{n}(x) \\ \hat{q}(x) \\ \hat{m}(x) \end{bmatrix} \mathrm{d}x, \tag{71}$$

with

$$\mathbf{K}(x,\xi) = \begin{bmatrix} \hat{N}^*(x,\xi) & 0 & 0 \\ 0 & \hat{Q}_q^*(x,\xi) & \hat{M}_q^*(x,\xi) \\ 0 & \hat{Q}_m^*(x,\xi) & \hat{M}_m^*(x,\xi) \end{bmatrix}, \quad \mathbf{u}(x) = \begin{bmatrix} \hat{u}(x) \\ \hat{w}(x) \\ \hat{\varphi}(x) \end{bmatrix}, \tag{72}$$

$$\mathbf{F}(x,\xi) = \begin{bmatrix} \hat{u}^*(x,\xi) & 0 & 0 \\ 0 & \hat{w}_q^*(x,\xi) & \hat{\varphi}_q^*(x,\xi) \\ 0 & \hat{w}_m^*(x,\xi) & \hat{\varphi}_m^*(x,\xi) \end{bmatrix}, \quad \mathbf{T}(x) = \begin{bmatrix} \hat{N}(x) \\ \hat{Q}(x) \\ \hat{M}(x) \end{bmatrix}. \tag{73}$$

Introducing the vectors $\mathbf{x}_0^{\mathrm{T}} = [\mathbf{u}(0), \mathbf{T}(0)]$, $\mathbf{x}_l^{\mathrm{T}} = [\mathbf{u}(l), \mathbf{T}(l)]$, the associated matrices

$$\mathbf{A} = \begin{bmatrix} \mathbf{I} - \mathbf{K}(0,0) & \mathbf{F}(0,0) \\ -\mathbf{K}(0,l) & \mathbf{F}(0,l) \end{bmatrix}, \quad \mathbf{B} = \begin{bmatrix} \mathbf{K}(l,0) & -\mathbf{F}(l,0) \\ \mathbf{K}(0,0) & -\mathbf{F}(0,0) \end{bmatrix}, \tag{74}$$

and the right side loading vector

$$\mathbf{r} = \begin{bmatrix} \mathbf{r}_0 \\ \mathbf{r}_l \end{bmatrix} = \int_0^l \begin{bmatrix} \mathbf{F}(x,0) \\ \mathbf{F}(x,l) \end{bmatrix} \begin{bmatrix} \hat{n}_x(x) \\ \hat{q}_z(x) \\ \hat{m}_y(x) \end{bmatrix} \mathrm{d}x, \tag{75}$$

the above system (71) can be given in the following short matrix-vector notation as

$$\mathbf{A}\mathbf{x}_0 + \mathbf{B}\mathbf{x}_l = \mathbf{r}. \tag{76}$$

Since in frames, the radiation condition is not important, it is advantageous to apply in the Laplace domain formulation the beam fundamental solutions (54)–(56) with their related states (A.1)–(A.4) and the bar fundamental solution (43) with the related axial resultant force (69). Then, the values at the singular points, i.e., for $r = 0$, are simply

$$\begin{aligned} &\hat{u}^*(0,0) = \hat{u}^*(l,l) = 0, \\ &\hat{w}_q^*(0,0) = \hat{w}_q^*(l,l) = 0, \quad \hat{\varphi}_q^*(0,0) = \hat{\varphi}_q^*(l,l) = 0, \\ &\hat{w}_m^*(0,0) = \hat{w}_m^*(l,l) = 0, \quad \hat{\varphi}_m^*(0,0) = \hat{\varphi}_m^*(l,l) = 0. \end{aligned} \tag{77}$$

$$\hat{N}^*(0,0) = -\hat{N}^*(l,l) = \frac{1}{2},$$
$$\hat{Q}_q^*(0,0) = -\hat{Q}_q^*(l,l) = \frac{1}{2}, \quad \hat{M}_q^*(0,0) = \hat{M}_q^*(l,l) = 0,$$
$$\hat{Q}_m^*(0,0) = \hat{Q}_m^*(l,l) = 0, \quad \hat{M}_m^*(0,0) = -\hat{M}_m^*(l,l) = \frac{1}{2}, \tag{78}$$

such that the sub-matrices related to $r = 0$ become:

$$\mathbf{K}(0,0) = -\mathbf{K}(l,l) = \begin{bmatrix} \frac{1}{2} & 0 & 0 \\ 0 & \frac{1}{2} & 0 \\ 0 & 0 & \frac{1}{2} \end{bmatrix}, \quad \mathbf{F}(0,0) = \mathbf{F}(l,l) = \begin{bmatrix} 0 & 0 & 0 \\ 0 & 0 & 0 \\ 0 & 0 & 0 \end{bmatrix} = \mathbf{0}. \tag{79}$$

Therefore, the system matrices (74) are reduced to

$$\mathbf{A} = \begin{bmatrix} \frac{1}{2}\mathbf{I} & \mathbf{0} \\ -\mathbf{K}(0,l) & \mathbf{F}(0,l) \end{bmatrix}, \quad \mathbf{B} = \begin{bmatrix} \mathbf{K}(l,0) & -\mathbf{F}(l,0) \\ \frac{1}{2}\mathbf{I} & \mathbf{0} \end{bmatrix}, \tag{80}$$

where for $r = l$, i.e., when the collocation point $\xi$ and the observation point $x$ are opposite to each other at end points of the beam and of the bar, respectively, the fundamental solution terms are all regular and, moreover, the following symmetry and antimetry relations, respectively, hold

$$\hat{u}^\infty(l,0) = \hat{u}^\infty(0,l),$$
$$\hat{w}_q^\infty(l,0) = \hat{w}_q^\infty(0,l), \quad \hat{\varphi}_q^\infty(l,0) = -\hat{\varphi}_q^\infty(0,l),$$
$$\hat{w}_m^\infty(l,0) = -\hat{w}_m^\infty(0,l), \quad \hat{\varphi}_m^\infty(l,0) = \hat{\varphi}_m^\infty(0,l), \tag{81}$$

$$\hat{N}^\infty(l,0) = -\hat{N}^\infty(0,l),$$
$$\hat{M}_q^\infty(l,0) = \hat{M}_q^\infty(0,l), \quad \hat{Q}_q^\infty(l,0) = -\hat{Q}_q^\infty(0,l),$$
$$\hat{M}_m^\infty(l,0) = -\hat{M}_m^\infty(0,l), \quad \hat{Q}_m^\infty(l,0) = \hat{Q}_m^\infty(0,l), \tag{82}$$

such that

$$\mathbf{F}(0,l) = \begin{bmatrix} \hat{u}^\infty(0,l) & 0 & 0 \\ 0 & \hat{w}_q^\infty(0,l) & \hat{\varphi}_q^\infty(0,l) \\ 0 & \hat{w}_m^\infty(0,l) & \hat{\varphi}_m^\infty(0,l) \end{bmatrix}, \tag{83}$$

$$\mathbf{F}(l,0) = \begin{bmatrix} \hat{u}^\infty(0,l) & 0 & 0 \\ 0 & \hat{w}_q^\infty(0,l) & -\hat{\varphi}_q^\infty(0,l) \\ 0 & -\hat{w}_m^\infty(0,l) & \hat{\varphi}_m^\infty(0,l) \end{bmatrix}, \tag{84}$$

$$\mathbf{K}(0,l) = \begin{bmatrix} \hat{N}^\infty(0,l) & 0 & 0 \\ 0 & \hat{Q}_q^\infty(0,l) & \hat{M}_q^\infty(0,l) \\ 0 & \hat{Q}_m^\infty(0,l) & \hat{M}_m^\infty(0,l) \end{bmatrix}, \tag{85}$$

$$\mathbf{K}(l,0)=\begin{bmatrix} -\hat{N}^{\infty}(0,l) & 0 & 0 \\ 0 & -\hat{Q}_q^{\infty}(0,l) & \hat{M}_q^{\infty}(0,l) \\ 0 & \hat{Q}_m^{\infty}(0,l) & -\hat{M}_m^{\infty}(0,l) \end{bmatrix}. \tag{86}$$

In the frequency domain, the fundamental solutions (35)–(38) with Eq. (A.5) for $\omega^2 > \kappa GA/\rho I$, i.e., $\lambda_1 < \lambda_2 < 0$, and Eqs. (57)–(59) with Eq. (A.6) for $\omega^2 < \kappa GA/\rho I$, i.e., $\lambda_1 < 0 < \lambda_2$, respectively, and consequently the fundamental states have at $x = \xi = 0$ and $x = \xi = l$, i.e. $r = 0$, the same behaviour as described above in Eqs. (77) and (78). Hence, the related sub-matrices become as given in Eq. (79).

The above system (76) of six equations holds for each structural frame part and relates the boundary values $\mathbf{x}_0^{\mathrm{T}} = [\mathbf{u}(0), \mathbf{T}(0)]$ at its beginning with the values $\mathbf{x}_l^{\mathrm{T}} = [\mathbf{u}(l), \mathbf{T}(l)]$ at its end. For modelling a complete frame, the systems for all frame parts have to be combined by adequate coupling conditions. This means here that the boundary values of those parts which shall be connected have to satisfy the equilibrium conditions for the respective axial forces $N$, the shear forces $Q$, and the bending moments $M$, while for the respective axial displacements $u$, the deflections $w$, and the rotations $\varphi$, the kinematic condition of adequate continuity has to be taken into account (for the detailed description of the rigid connection of two or more parts, see Appendix B).

This is different from the classical displacement-based FEM where only the kinematic conditions are satisfied.

### 4.4. Time domain solution by the Convolution Quadrature Method

To obtain a time-dependent integral equation, a formal inverse Laplace transformation has to be applied on Eq. (65) for the beam and on Eq. (68). Every product there is changed to a convolution with respect to time resulting in

$$\begin{aligned} \begin{bmatrix} w(\xi,t) \\ \varphi(\xi,t) \\ u(\xi,t) \end{bmatrix} = {} & \int_0^t \int_0^{\ell} \begin{bmatrix} w_q^*(x,\xi,t-\tau) & w_m^*(x,\xi,t-\tau) & 0 \\ \varphi_q^*(x,\xi,t-\tau) & \varphi_m^*(x,\xi,t-\tau) & 0 \\ 0 & 0 & u^*(x,\xi,t-\tau) \end{bmatrix}^{\mathrm{T}} \begin{bmatrix} q(x,\tau) \\ m(x,\tau) \\ n(x,\tau) \end{bmatrix} \mathrm{d}x\,\mathrm{d}\tau \\ & + \int_0^t \left( \begin{bmatrix} w_q^*(x,\xi,t-\tau) & w_m^*(x,\xi,t-\tau) & 0 \\ \varphi_q^*(x,\xi,t-\tau) & \varphi_m^*(x,\xi,t-\tau) & 0 \\ 0 & 0 & u^*(x,\xi,t-\tau) \end{bmatrix}^{\mathrm{T}} \begin{bmatrix} Q(x,\tau) \\ M(x,\tau) \\ N(x,\tau) \end{bmatrix} \right. \\ & \left. - \begin{bmatrix} Q_q^*(x,\xi,t-\tau) & Q_m^*(x,\xi,t-\tau) & 0 \\ M_q^*(x,\xi,t-\tau) & M_m^*(x,\xi,t-\tau) & 0 \\ 0 & 0 & N^*(x,\xi,t-\tau) \end{bmatrix}^{\mathrm{T}} \begin{bmatrix} w(x,\tau) \\ \varphi(x,\tau) \\ u(\xi,\tau) \end{bmatrix} \right]_{x=0}^{x=\ell} \mathrm{d}\tau. \end{aligned} \tag{87}$$

Hence, time-dependent fundamental solutions are needed. Due to the lack of these solutions in a computational effective form, the convolution quadrature method proposed by

Lubich [17,18] ($n = 0, 1, \ldots, N$)

$$y(t) = \int_0^t f(t-\tau)g(\tau)\,\mathrm{d}\tau \Rightarrow y(n\Delta t) = \sum_{k=0}^{n} \omega_{n-k}(\hat{f}, \Delta t)g(k\Delta t), \tag{88}$$

with the integration weights

$$\omega_n(\hat{f}, \Delta t) = \frac{\mathscr{R}^{-n}}{L} \sum_{\ell=0}^{L-1} \hat{f}\left(\frac{\gamma(\mathscr{R}\mathrm{e}^{\mathrm{i}\ell 2\pi/L})}{\Delta t}\right)\mathrm{e}^{-\mathrm{i}n\ell 2\pi/L}, \tag{89}$$

is used. A brief overview of this method can be found in Appendix C. In Eq. (88), the time $t$ is discretized in $N$ time steps of equal duration $\Delta t$, and $\gamma(z)$ denotes the quotient of characteristic polynomials of the underlying multi-step method. In the following, a backward differential formula of order two will be used as well as the choice $L = N$.

Applying this quadrature rule on Eq. (87), a time-stepping procedure for $n = 0, 1, \ldots, N$ is achieved

$$\begin{aligned}
\begin{bmatrix} w(\xi,\Delta t) \\ \varphi(\xi,\Delta t) \\ u(\xi,\Delta t) \end{bmatrix} = {} & \sum_{k=0}^{n} \int_0^{\ell} \omega_{n-k}\left(\begin{bmatrix} \hat{w}_q^*(x,\xi) & \hat{w}_m^*(x,\xi) & 0 \\ \hat{\varphi}_q^*(x,\xi) & \hat{\varphi}_m^*(x,\xi) & 0 \\ 0 & 0 & \hat{u}^*(x,\xi) \end{bmatrix}^{\mathrm{T}}, \Delta t\right) \begin{bmatrix} q(x,k\Delta t) \\ m(x,k\Delta t) \\ n(x,k\Delta t) \end{bmatrix} \mathrm{d}x \\
& + \sum_{k=0}^{n} \left[ \omega_{n-k}\left(\begin{bmatrix} \hat{w}_q^*(x,\xi) & \hat{w}_m^*(x,\xi) & 0 \\ \hat{\varphi}_q^*(x,\xi) & \hat{\varphi}_m^*(x,\xi) & 0 \\ 0 & 0 & \hat{u}^*(x,\xi) \end{bmatrix}^{\mathrm{T}}, \Delta t\right) \begin{bmatrix} Q(x,k\Delta t) \\ M(x,k\Delta t) \\ N(x,k\Delta t) \end{bmatrix} \right. \\
& \left. - \omega_{n-k}\left(\begin{bmatrix} \hat{Q}_q^*(x,\xi) & \hat{Q}_m^*(x,\xi) & 0 \\ \hat{M}_q^*(x,\xi) & \hat{M}_m^*(x,\xi) & 0 \\ 0 & 0 & \hat{N}^*(x,\xi) \end{bmatrix}^{\mathrm{T}}, \Delta t\right) \begin{bmatrix} w(x,k\Delta t) \\ \varphi(x,k\Delta t) \\ u(\xi,k\Delta t) \end{bmatrix} \right]_{x=0}^{x=\ell}
\end{aligned} \tag{90}$$

whereas the discontinuous behaviour (78) can be transferred to the time domain.

Note, with the quadrature rule (88) only Laplace transformed fundamental solutions are required to obtain the time-stepping procedure (90). Remarks on proper choices of the parameters $L, \mathscr{R}, \gamma(z), \Delta t$ may be found in Ref. [19].

One remark must be added on the fundamental solution for the beam equation. In Sections 3.1 and 3.3, two different fundamental solutions are given. The first, solution (27) tends to zero for large distances $r$ as well as large frequencies $\omega$ but does not yield the static solution in the limit $\omega \to 0$. Conversely, solution (53) has a proper limit to the static case but does not tend to zero for large distances $r$. In principle, in the time domain solution of the frame both fundamental solutions lead to good results, however, solution (53) is very sensitive on choosing the time step size $\Delta t$. So, here, the other solution (27) must be used to get a stable algorithm. Also, in the time domain there is no necessity that the solution tends to the static solution for small frequencies.

## 5. Examples

Two examples are presented to demonstrate the method's exactness compared with finite element results. First, a single straight beam where the shift of the resonance frequencies when using the Timoshenko theory instead of Euler–Bernoulli's theory is shown, and, second, a two-storey framework where, in addition to the frequency response, the causality of a propagating wave is studied.

### 5.1. Straight beam

A straight steel beam (Young's modulus $E = 2.1 \times 10^{11}$ N/m$^2$, Poisson's ratio $v = 0.3$, and material density $\rho = 7850$ kg/m$^3$) of length $l = 1$ m and rectangular cross-section $A$ with $b = h = 0.1$ m is considered taking the shear correction factor $\kappa = 5/6$. It is subjected to a harmonic lateral point loading with frequency $\omega$ ($\omega^2 < \kappa GA/\rho I \approx 20.58 \times 10^8$(rad/s)$^2$, i.e., $\omega < 4.53 \times 10^4$ rad/s $\approx 7.2 \times 10^3$ Hz) acting at $x = l/2$ with constant amplitude $q_0$, i.e., $\hat{q}(x) = q_0\delta(x - l/2)$. Its boundaries are assumed to be fixed at $x = 0$, i.e., $u(0) = w(0) = \varphi(0) = 0$, and simply supported at $x = l$, i.e., $u(l) = w(l) = M(l) = 0$ (see, Fig. 1). Taking these conditions into account, system (71) and (76), respectively, with the fundamental solutions (54)–(56) and (49) as well as with Eqs. (57)–(59) and (70), i.e., with the matrices (80) is reduced to

$$\begin{bmatrix} 0 & 0 & 0 & 0 & -\hat{u}^*(l,0) & 0 \\ 0 & 0 & 0 & \hat{M}_q^*(l,0) & 0 & -\hat{w}_q^*(l,0) \\ 0 & 0 & 0 & \hat{M}_m^*(l,0) & 0 & -\hat{w}_m^*(l,0) \\ \hat{u}^*(0,l) & 0 & 0 & 0 & 0 & 0 \\ 0 & \hat{w}_q^*(0,l) & \hat{\varphi}_q^*(0,l) & 0 & 0 & 0 \\ 0 & \hat{w}_m^*(0,l) & \hat{\varphi}_m^*(0,l) & \frac{1}{2} & 0 & 0 \end{bmatrix} \begin{bmatrix} N(0) \\ Q(0) \\ M(0) \\ \varphi(l) \\ N(l) \\ Q(l) \end{bmatrix} = \begin{bmatrix} 0 \\ q_{0q} \\ q_{0m} \\ 0 \\ q_{0q} \\ -q_{0m} \end{bmatrix}, \quad (91)$$

where, due to the filtering effect of the $\delta(x - l/2)$ term, the right side integrals can easily be evaluated as

$$q_{0q} = q_0\hat{w}_q^*\left(\frac{l}{2}, 0\right) = q_0\hat{w}_q^*\left(\frac{l}{2}, l\right), \quad (92)$$

$$q_{0m} = q_0\hat{w}_m^*\left(\frac{l}{2}, 0\right) = -q_0\hat{w}_m^*\left(\frac{l}{2}, l\right). \quad (93)$$

The first and the fourth equations give $N(l) = 0$ and $N(0) = 0$. Then, from the second and third equations, one can easily find

$$\varphi(l) = q_0 \frac{\hat{w}_q^*\left(\frac{l}{2}, 0\right)\hat{w}_m^*(l,0) - \hat{w}_m^*\left(\frac{l}{2}, 0\right)\hat{w}_q^*(l,0)}{\hat{M}_q^*(l,0)\hat{w}_m^*(l,0) - \hat{M}_m^*(l,0)\hat{w}_q^*(l,0)}, \quad (94)$$

$$Q(l) = q_0 \frac{\hat{w}_q^*\left(\frac{l}{2}, 0\right)\hat{M}_m^*(l,0) - \hat{w}_m^*\left(\frac{l}{2}, 0\right)\hat{M}_q^*(l,0)}{\hat{M}_q^*(l,0)\hat{w}_m^*(l,0) - \hat{M}_m^*(l,0)\hat{w}_q^*(l,0)}, \quad (95)$$

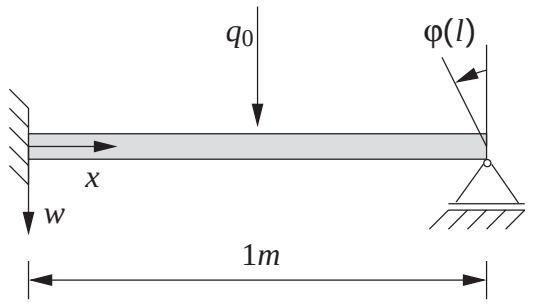


Fig. 1. Straight fixed–simply supported beam: geometry and loading.

and, finally, from the fifth and sixth equations (with $\hat{w}_m^*(0,l) = -\hat{w}_m^*(l,0)$, $\hat{w}_q^*(0,l) = \hat{w}_q^*(l,0)$, $\hat{\varphi}_q^*(0,l) = -\hat{\varphi}_q^*(l,0)$, $\hat{\varphi}_m^*(0,l) = \hat{\varphi}_m^*(l,0)$)

$$M(0) = \frac{q_0\left[\hat{w}_m^*\left(\frac{l}{2},0\right)\hat{w}_q^*(l,0) - \hat{w}_q^*\left(\frac{l}{2},0\right)\hat{w}_m^*(l,0)\right] + \frac{1}{2}\hat{w}_q^*(l,0)\varphi(l)}{\hat{\varphi}_q^*(l,0)\hat{w}_m^*(l,0) - \hat{\varphi}_m^*(l,0)\hat{w}_q^*(l,0)}, \tag{96}$$

$$Q(0) = \frac{q_0\left[\hat{w}_m^*\left(\frac{l}{2},0\right)\hat{\varphi}_q^*(l,0) - \hat{w}_q^*\left(\frac{l}{2},0\right)\hat{\varphi}_m^*(l,0)\right] + \frac{1}{2}\hat{\varphi}_q^*(l,0)\varphi(l)}{\hat{\varphi}_q^*(l,0)\hat{w}_m^*(l,0) - \hat{\varphi}_m^*(l,0)\hat{w}_q^*(l,0)}. \tag{97}$$

With these boundary reactions, the integral equations (76) give the deflection and the rotation, respectively, at any interior point and for all excitation frequencies $\omega$ ($\omega^2 < \kappa GA/\rho I_y$; for higher frequencies, only the respective other fundamental solution must be used), e.g,

$$w(\xi) = q_0\hat{w}_q^*\left(\frac{l}{2},\xi\right) + \hat{w}_q^*(l,\xi)Q(l) - \hat{M}_q^*(l,\xi)\varphi(l) - \hat{w}_q^*(0,\xi)Q(0) - \hat{\varphi}_q^*(0,\xi)M(0). \tag{98}$$

An evaluation of the frequency dependence of these boundary reactions (94)–(97), e.g., of the rotation $\varphi(l)$ shows that the exact solution from the boundary integral formulation is only approximately reached by a finite element approach (applying cubic Lagrange functions, i.e., a 4-node element with static condensation which means four-degrees-of-freedom per element; for details, see Ref. [28]) when about 20 elements are used (see, Fig. 2). Solving the same problem in the Euler–Bernoulli beam theory, i.e., applying the boundary integral equation formulation and the finite element approach with $D_1 = \kappa GA \to \infty$, shows (see, Fig. 3) again, the finite element results converge to the exact boundary integral solution. Moreover, when comparing the Timoshenko theory and the Euler–Bernoulli theory results, a shift of all resonance frequencies becomes obvious: the shift is larger, the higher the resonance frequency (see Table 1).

### 5.2. Plane frame

As a second, more complicated example, a plane framework is considered which consists of six rigidly connected beams with the same material data as in the first example. The excitation is again a frequency-dependent point load of intensity $q_0 = 1000$ N acting at the centre of the top

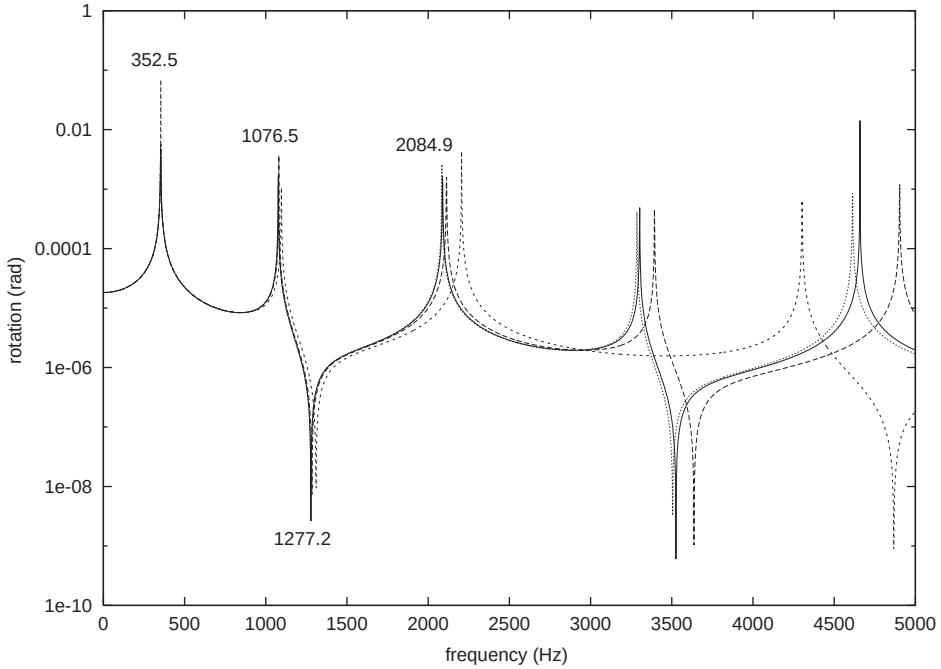


Fig. 2. Frequency dependence of the beam end rotation: comparison of BEM and FEM Timoshenko beam results. ———, FEM (20 elements); — — —, FEM (8 elements); - - - - -, FEM (4 elements); ·····, BEM.

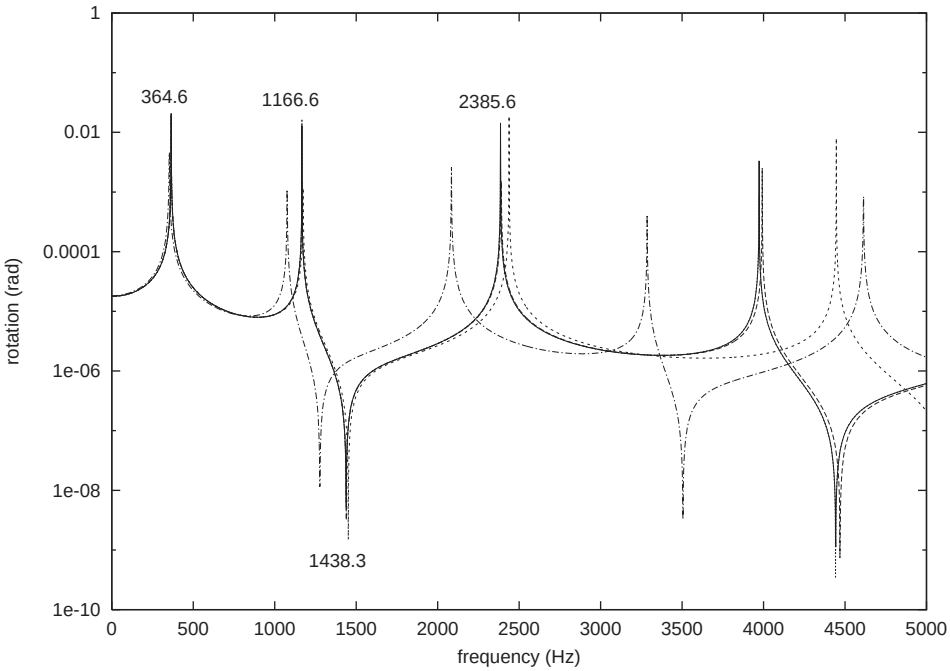


Fig. 3. Frequency dependence of the beam end rotation: comparison of BEM and FEM Euler–Bernoulli beam results and shift of resonance frequencies in Timoshenko's theory. ——, FEM (20 elements); — — —, FEM (8 elements); - - - - -, FEM (4 elements); ·····, BEM (Euler–Bernoulli theory); – · –·, BEM (Timoshenko theory).

Table 1
Shift of resonance frequencies in Timoshenko theory compared to Euler–Bernoulli theory

| | Resonance frequency (Hz) | | | |
|---|---|---|---|---|
| | 1st | 2nd | 3rd | 4th |
| Euler–Bernoulli theory | 364.6 | 1166.6 | 1438.3 | 2385.6 |
| Timoshenko theory | 352.5 | 1076.5 | 1277.2 | 2084.9 |

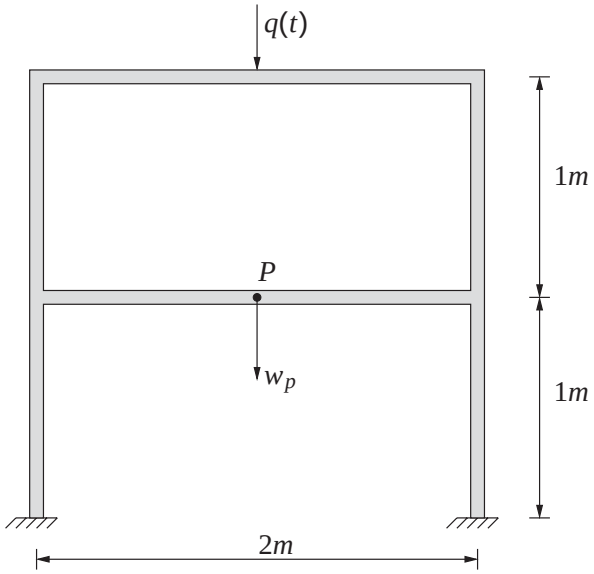


Fig. 4. Plane frame of six rigidly fixed beams: geometry, support, and loading.

beam (see Fig. 4) and the whole two-storey building model is rigidly fixed in rigid soil. A mapping (Fig. 5) of the deflection response $w_P$ at the centre point $P$ on the first frame floor for excitations up to 1600 Hz (increasing the excitation frequency in steps of 10 rad/s$\approx$1.6 Hz) from both formulations, the Timoshenko boundary integral equations and finite element approximations with 32 and 64 elements, respectively, and cubic shape functions (see, above) shows an excellent agreement up to about 700 Hz. In order to demonstrate the accuracy of the Convolution Quadrature Method for the analysis of the waves propagating along the frame beams, its results are compared with a finite element solution found by using the commercial software NASTRAN with 24, 40, and 80 elements assuming an impact load $q = q_0 H(t)$ N/m with constant intensity $q_0$ ($H(t)$ denotes the Heaviside function). Considering the time history of, e.g., the deflection $w_P(t)$ at centre point $P$ on the first frame floor (Fig. 6) during the initial 0.075 s, i.e., during 750 time steps $\Delta t = 0.0001$ s, shows on the whole an almost perfect coincidence of the boundary integral equation result and of the finite element solution. This is also true with respect to the causality condition: since the wave speeds in the steel beams are $c_1 = 5172$ m/s and $c_2 = 2928$ m/s, the

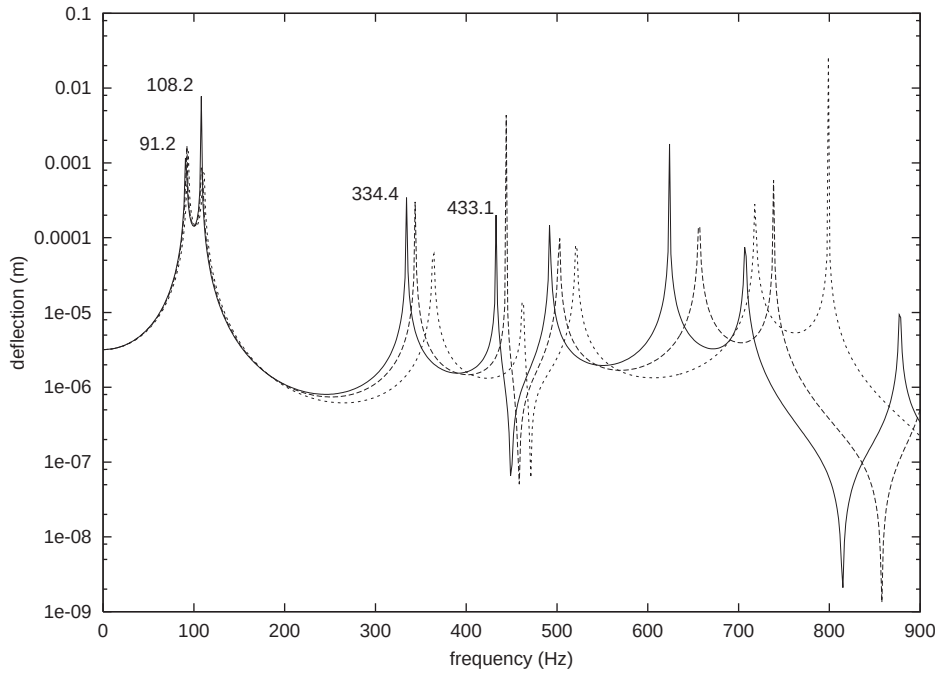


Fig. 5. Frequency dependence of the deflection at point P: comparison of Timoshenko BEM and FEM results. ———, BEM; — — —, FEM 64 elements; - - - - -, FEM 32 elements.

faster longitudinal wave should propagate the 3 m distance from the excitation point to the point $P$ in 0.00058 s and the slower shear wave should arrive after 0.00102 s. But, due to the fact that waves arrive at $P$ from the left side and from the right side at the same time, the two longitudinal waves cancel each other, and only the arrival of the shear wave is visible in the boundary integral solution. Hence, in the first 0.00102 s the response has to be identically zero. This is obviously satisfied by the boundary integral equation (BEM) results and for the FEM solution (NASTRAN) when at least 40 elements are applied (see, Fig. 7).

## 6. Conclusions

Considering vibrating beams in the Laplace domain and for harmonic excitations, fundamental solutions for the second order differential equation system of Timoshenko's theory, i.e., the deflection $w$ and the rotation $\varphi_y$ due to a unit point force as well as to a unit single moment around the $y$-axis are derived. Then, starting from the residua of the basic differential equations weighted by these fundamental solutions, integral equations are formulated for deflection and rotation. It should be mentioned that the Euler–Bernoulli beam representation is contained as a special case.

Point collocation at the beam's endings gives a system of equations which delivers the unknown boundary reactions exactly. With these boundary values, the integral equations are exact

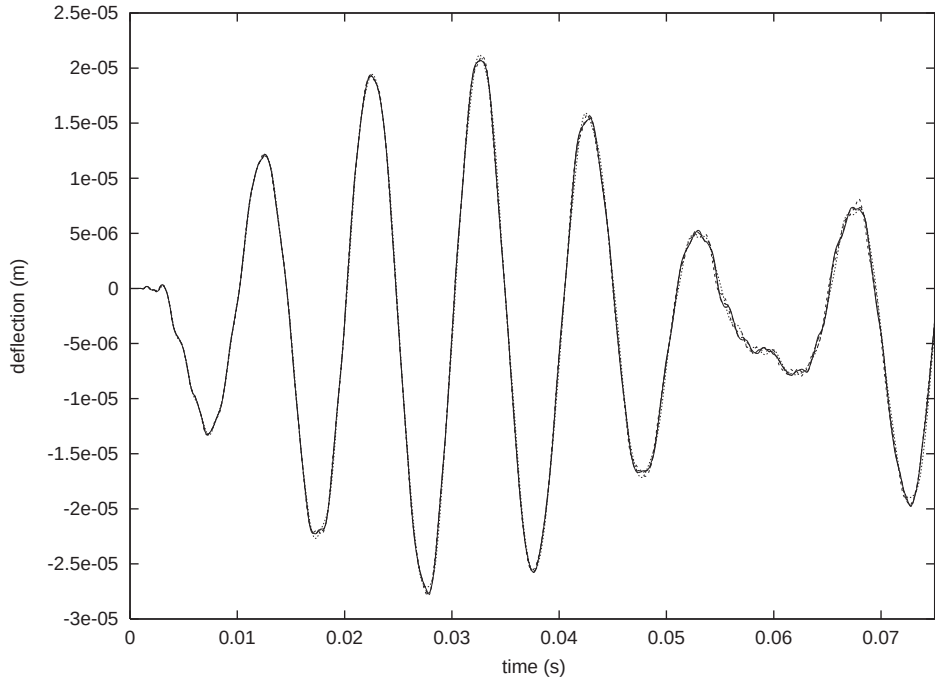


Fig. 6. Time history of the deflection at point P: comparison of Timoshenko BEM and NASTRAN-FEM results. ———, MSC Nastran 80 elements; — — —, MSC Nastran 40 elements; - - - - -, MSC Nastran 24 elements; ·····, BEM.

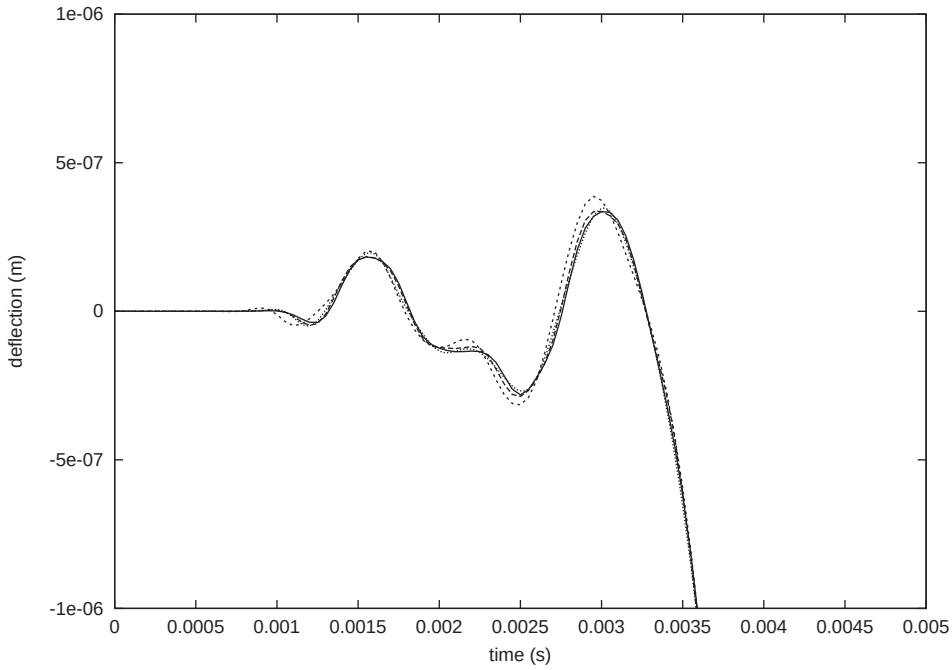


Fig. 7. Time history of the deflection at point P: causality check of Timoshenko BEM and NASTRAN-FEM results. ———, MSC Nastran 80 elements; — — —, MSC Nastran 40 elements; - - - - -, MSC Nastran 24 elements; ·····, BEM.

analytical representations of the deflection and the rotation dynamic behaviour at any point. This is different to corresponding finite element solutions where the accuracy depends, both on the number of elements, and on the adequacy of the applied shape functions with respect to the actual loadings.

Applying the convolution quadrature method to the Laplace domain integral equations produces the time domain solution, i.e., wave propagation process.

The correctness of the formulations is checked by two representative examples where the boundary integral equation solutions are compared to finite element method results: a single beam where the shift of the resonance frequencies when using the Timoshenko theory instead of Euler–Bernoulli's theory is shown, and a two-storey framework where, in addition to the frequency response, the causality behaviour of the propagating wave is studied. In both examples, the finite element method results coincide with the boundary integral equation solutions if enough elements are applied.

## Appendix A. Shear force and bending moment of fundamental solutions

As already mentioned before, it is convenient for finite beams (where the radiation condition is not important) to take the fundamental solutions (54)–(56) for the Laplace domain integral equations. The corresponding shear forces and bending moments are

$$\hat{Q}_q^*(x,\xi) = \frac{r_{,x}}{2(\lambda_2-\lambda_1)}\left[\left(\lambda_1 - \frac{S_2}{D_2}\right)\cosh\left(\sqrt{\lambda_1}r\right) - \left(\lambda_2 - \frac{S_2}{D_2}\right)\cosh\left(\sqrt{\lambda_2}r\right)\right], \tag{A.1}$$

$$\hat{M}_q^*(x,\xi) = \frac{1}{2(\lambda_2-\lambda_1)}\left[\sqrt{\lambda_1}\sinh\left(\sqrt{\lambda_1}r\right) - \sqrt{\lambda_2}\sinh\left(\sqrt{\lambda_2}r\right)\right], \tag{A.2}$$

and

$$\hat{Q}_m^*(x,\xi) = \frac{-S_1}{2D_2(\lambda_2-\lambda_1)}\left[\frac{\sinh\left(\sqrt{\lambda_1}r\right)}{\sqrt{\lambda_1}} - \frac{\sinh\left(\sqrt{\lambda_2}r\right)}{\sqrt{\lambda_2}}\right], \tag{A.3}$$

$$\hat{M}_m^*(x,\xi) = \frac{r_{,x}}{2(\lambda_2-\lambda_1)}\left[\left(\lambda_1 - \frac{S_1}{D_1}\right)\cosh\left(\sqrt{\lambda_1}r\right) - \left(\lambda_2 - \frac{S_1}{D_1}\right)\cosh\left(\sqrt{\lambda_2}r\right)\right]. \tag{A.4}$$

In the frequency domain, the integral equation system is formally identical (65), but the solutions are different and, moreover, dependent on the size of the excitation frequency $\omega$, i.e., Eqs. (35)–(38) for $\omega^2 > \kappa GA/\rho I$ and Eqs. (57)–(59) for $\omega^2 < \kappa GA/\rho I$. Hence, the corresponding shear forces and bending moments are ($S_1/D_1 = -\omega^2/c_2^2,\ S_2/D_2 = -\omega^2/c_1^2$):

for $\omega^2 > \kappa GA/\rho I$, i.e., $\lambda_1 < \lambda_2 < 0$:

$$\hat{Q}_q^*(x,\xi) = \frac{r_{,x}}{2(\lambda_2-\lambda_1)}\left[\left(\lambda_1 - \frac{S_2}{D_2}\right)\cos\left(\sqrt{-\lambda_1}r\right) - \left(\lambda_2 - \frac{S_2}{D_2}\right)\cos\left(\sqrt{-\lambda_2}r\right)\right],$$

$$\hat{M}_q^*(x,\xi) = \frac{-1}{2(\lambda_2-\lambda_1)}\left[\sqrt{-\lambda_1}\sin\left(\sqrt{-\lambda_1}r\right) - \sqrt{-\lambda_2}\sin\left(\sqrt{-\lambda_2}r\right)\right],$$

$$\hat{Q}_m^*(x,\xi) = \frac{-S_1}{2D_2(\lambda_2-\lambda_1)}\left[\frac{\sin\left(\sqrt{-\lambda_1}r\right)}{\sqrt{-\lambda_1}} - \frac{\sin\left(\sqrt{-\lambda_2}r\right)}{\sqrt{-\lambda_2}}\right],$$

$$\hat{M}_m^*(x,\xi) = \frac{r_{,x}}{2(\lambda_2-\lambda_1)}\left[\left(\lambda_1 - \frac{S_1}{D_1}\right)\cos\left(\sqrt{-\lambda_1}r\right) - \left(\lambda_2 - \frac{S_1}{D_1}\right)\cos\left(\sqrt{-\lambda_2}r\right)\right]; \qquad \text{(A.5)}$$

for $\omega^2 < \kappa GA/\rho I$, i.e., $\lambda_1 < 0 < \lambda_2$:

$$\hat{Q}_q^*(x,\xi) = \frac{r_{,x}}{2(\lambda_2-\lambda_1)}\left[\left(\lambda_1 - \frac{S_2}{D_2}\right)\cos\left(\sqrt{-\lambda_1}r\right) - \left(\lambda_2 - \frac{S_2}{D_2}\right)\cosh\left(\sqrt{\lambda_2}r\right)\right],$$

$$\hat{M}_q^*(x,\xi) = \frac{-1}{2(\lambda_2-\lambda_1)}\left[\sqrt{-\lambda_1}\sin\left(\sqrt{-\lambda_1}r\right) + \sqrt{\lambda_2}\sinh\left(\sqrt{\lambda_2}r\right)\right],$$

$$\hat{Q}_m^*(x,\xi) = \frac{-S_1}{2D_2(\lambda_2-\lambda_1)}\left[\frac{\sin\left(\sqrt{-\lambda_1}r\right)}{\sqrt{-\lambda_1}} - \frac{\sinh\left(\sqrt{\lambda_2}r\right)}{\sqrt{\lambda_2}}\right],$$

$$\hat{M}_m^*(x,\xi) = \frac{r_{,x}}{2(\lambda_2-\lambda_1)}\left[\left(\lambda_1 - \frac{S_1}{D_1}\right)\cos\left(\sqrt{-\lambda_1}r\right) - \left(\lambda_2 - \frac{S_1}{D_1}\right)\cosh\left(\sqrt{\lambda_2}r\right)\right]. \qquad \text{(A.6)}$$

## Appendix B. Rigid connection of frame parts

The most common type of connections in frames is certainly the rigid connection (see Fig. 8). When the local longitudinal axis $x^i$ and $x^{i+1}$ of two subsequent frame parts $\Omega_i$ and $\Omega_{i+1}$ have angles $\alpha^i$ and $\alpha^{i+1}$, respectively, to the global horizontal axis $x_1$, i.e., there is an angle change of $\Delta\alpha_i^{i+1} = \alpha^{i+1} - \alpha^i$, and the two frame parts are rigidly fixed to each other, the boundary values at the connection point, i.e., at the end point $x^i = l_i$ of part $\Omega_i$ and at the initial point $x^{i+1} = 0$ of part $\Omega_{i+1}$, are coupled via the dynamic conditions

$$\begin{bmatrix} \hat{N}^i(l_i) \\ \hat{Q}^i(l_i) \\ \hat{M}^i(l_i) \end{bmatrix} = \begin{bmatrix} \cos\Delta\alpha_i^{i+1} & \sin\Delta\alpha_i^{i+1} & 0 \\ -\sin\Delta\alpha_i^{i+1} & \cos\Delta\alpha_i^{i+1} & 0 \\ 0 & 0 & 1 \end{bmatrix} \begin{bmatrix} \hat{N}^{i+1}(0) \\ \hat{Q}^{i+1}(0) \\ \hat{M}^{i+1}(0) \end{bmatrix}, \quad \text{i.e., } \mathbf{T}^i(l_i) = \mathbf{C}_i^{i+1} \cdot \mathbf{T}^{i+1}(0), \qquad \text{(B.1)}$$

and the kinematic conditions

$$\begin{bmatrix} \hat{u}^{i+1}(0) \\ \hat{w}^{i+1}(0) \\ \hat{\varphi}^{i+1}(0) \end{bmatrix} = \begin{bmatrix} \cos\Delta\alpha_i^{i+1} & -\sin\Delta\alpha_i^{i+1} & 0 \\ \sin\Delta\alpha_i^{i+1} & \cos\Delta\alpha_i^{i+1} & 0 \\ 0 & 0 & 1 \end{bmatrix} \begin{bmatrix} \hat{u}^i(l_i) \\ \hat{w}^i(l_i) \\ \hat{\varphi}^i(l_i) \end{bmatrix}, \quad \text{i.e., } \mathbf{u}^{i+1}(0) = [\mathbf{C}_i^{i+1}]^{-1} \cdot \mathbf{u}^i(l_i). \qquad \text{(B.2)}$$

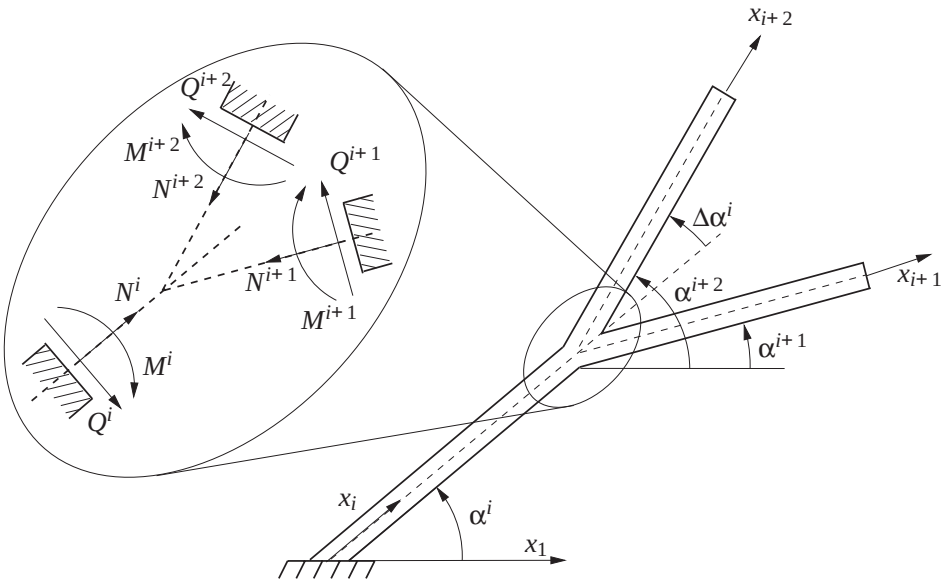


Fig. 8. Coupling of three beam endings: definition of inclination angles, axial and lateral forces, and bending moments.

Applying these coupling conditions gives the following system for two rigidly connected frame parts (here, the index of $l_i$ is neglected when it is obvious that $l$ means the beam length of the respective part $\Omega_i$):

$$\mathbf{A}^i \cdot \mathbf{x}_0^i + \mathbf{B}^i \cdot \overset{\langle \mathrm{T} \rangle}{\mathbf{C}}_{i,i+1} \cdot \mathbf{x}_{cr}^{i,i+1} = \mathbf{r}^i, \tag{B.3}$$

$$\mathbf{A}^{i+1} \overset{\langle 2u \rangle}{\mathbf{C}}{}_i^{i+1} \cdot \mathbf{x}_{cr}^{i,i+1} + \mathbf{B}^{i+1} \cdot \mathbf{x}_l^{i+1} = \mathbf{r}^{i+1}, \tag{B.4}$$

or in a block-matrix notation

$$\begin{bmatrix} \mathbf{A}^i & \mathbf{B}^i \cdot \overset{\langle \mathrm{T} \rangle}{\mathbf{C}}_{i,i+1} & \mathbf{0} \\ \mathbf{0} & \mathbf{A}^{i+1} \cdot \overset{\langle 2u \rangle}{\mathbf{C}}{}_i^{i+1} & \mathbf{B}^{i+1} \end{bmatrix} \cdot \begin{bmatrix} \mathbf{x}_0^i \\ \mathbf{x}_{cr}^{i,i+1} \\ \mathbf{x}_l^{i+1} \end{bmatrix} = \begin{bmatrix} \mathbf{r}^i \\ \mathbf{r}^{i+1} \end{bmatrix}, \tag{B.5}$$

where the vector $\mathbf{x}_{cr}^{i,i+1}$ contains the remaining unknown states at the rigid connection while the matrices $\overset{\langle \mathrm{T} \rangle}{\mathbf{C}}_{i,i+1}$ and $\overset{\langle 2u \rangle}{\mathbf{C}}{}_i^{i+1}$ realize the dynamic conditions and the kinematic conditions for the rigid coupling of two frame members:

$$\mathbf{x}_{cr}^{i,i+1} = \begin{bmatrix} \mathbf{u}^i(l) \\ \mathbf{T}^{i+1}(0) \end{bmatrix}, \quad \overset{\langle \mathrm{T} \rangle}{\mathbf{C}}_{i,i+1} = \begin{bmatrix} \mathbf{I} & \mathbf{0} \\ \mathbf{0} & \mathbf{C}_i^{i+1} \end{bmatrix}, \quad \overset{\langle 2u \rangle}{\mathbf{C}}{}_i^{i+1} = \begin{bmatrix} [\mathbf{C}_i^{i+1}]^{-1} & \mathbf{0} \\ \mathbf{0} & \mathbf{I} \end{bmatrix}. \tag{B.6}$$

In more detail, the coefficient matrix of Eq. (B.5) is as follows:

$$\begin{bmatrix} \frac{1}{2}\mathbf{I} & \mathbf{0} & \mathbf{K}^i(l,0) & -\mathbf{F}^i(l,0)\cdot\mathbf{C}_i^{i+1} & \mathbf{0} & \mathbf{0} \\ -\mathbf{K}^i(0,l) & \mathbf{F}^i(0,l) & \frac{1}{2}\mathbf{I} & \mathbf{0} & \mathbf{0} & \mathbf{0} \\ \mathbf{0} & \mathbf{0} & \frac{1}{2}[\mathbf{C}_i^{i+1}]^{-1} & \mathbf{0} & \mathbf{K}^{i+1}(l,0) & -\mathbf{F}^{i+1}(l,0) \\ \mathbf{0} & \mathbf{0} & -\mathbf{K}^{i+1}(0,l)\cdot[\mathbf{C}_i^{i+1}]^{-1} & \mathbf{F}^{i+1}(0,l) & \frac{1}{2}\mathbf{I} & \mathbf{0} \end{bmatrix}. \tag{B.7}$$

When three beam/bar parts of the framework, additional to $\Omega_i$ and $\Omega_{i+1}$ a part $\Omega_j$, shall be rigidly connected where the end point $x^i = l_i$ of $\Omega_i$ is coupled with the initial points $x^{i+1} = 0$ of $\Omega_{i+1}$ and $x^j = 0$ of $\Omega_j$, the above coupling conditions (B.1) and (B.2) have to be extended: The dynamic equilibrium condition (B.1) now reads for connecting the end point of $\Omega_i$ with two initial points, that of $\Omega_{i+1}$ and that of $\Omega_j$

$$\mathbf{T}^i(l_i) = \mathbf{C}_i^{i+1}\cdot\mathbf{T}^{i+1}(0) + \mathbf{C}_i^{j}\cdot\mathbf{T}^{j}(0), \tag{B.8}$$

while the kinematic continuity condition (B.2) gives an extra coupling system for each extra part

$$\mathbf{u}^{i+1}(0) = [\mathbf{C}_i^{i+1}]^{-1}\cdot\mathbf{u}^i(l_i), \tag{B.9}$$

$$\mathbf{u}^{j}(0) = [\mathbf{C}_i^{j}]^{-1}\cdot\mathbf{u}^i(l_i). \tag{B.10}$$

Applying these conditions gives the following system for the coupled three-part frame

$$\begin{bmatrix} \mathbf{A}^i & \mathbf{B}^i\cdot{}^{\langle \mathrm{T}\rangle}\mathbf{C}^{ebb}_{i,i+1,i+2} & \mathbf{0} & \mathbf{0} \\ \mathbf{0} & \mathbf{A}^{i+1}\cdot{}^{\langle 3u\rangle}\mathbf{C}^{\ }_{i\ i+1} & \mathbf{B}^{i+1} & \mathbf{0} \\ \mathbf{0} & \mathbf{A}^{j}\,{}^{\langle 3u\rangle}\mathbf{C}^{\ }_{j\ i} & \mathbf{0} & \mathbf{B}^{j} \end{bmatrix} \cdot \begin{bmatrix} \mathbf{x}_0^i \\ \mathbf{x}_{cr}^{i,i+1,j} \\ \mathbf{x}_l^{i+1} \\ \mathbf{x}_l^{j} \end{bmatrix} = \begin{bmatrix} \mathbf{r}^i \\ \mathbf{r}^{i+1} \\ \mathbf{r}^{j} \end{bmatrix}, \tag{B.11}$$

where the vector $\mathbf{x}_{cr}^{i,i+1,j}$ containing the remaining unknown states at the rigid connection and the essential coupling matrices are here

$$\mathbf{x}_{cr}^{i,i+1,i+2j} = \begin{bmatrix} \mathbf{u}^i(l) \\ \mathbf{T}^{i+1}(0) \\ \mathbf{T}^{j}(0) \end{bmatrix}, \quad {}^{\langle \mathrm{T}\rangle}\mathbf{C}^{ebb}_{i,i+1,j} = \begin{bmatrix} \mathbf{I} & \mathbf{0} & \mathbf{0} \\ \mathbf{0} & \mathbf{C}_i^{i+1} & \mathbf{C}_i^{j} \end{bmatrix}, \tag{B.12}$$

$${}^{\langle 3u\rangle}\mathbf{C}^{\ }_{i\ i+1} = \begin{bmatrix} [\mathbf{C}_i^{i+1}]^{-1} & \mathbf{0} & \mathbf{0} \\ \mathbf{0} & \mathbf{I} & \mathbf{0} \end{bmatrix}, \quad {}^{\langle 3u\rangle}\mathbf{C}^{\ }_{j\ i} = \begin{bmatrix} [\mathbf{C}_i^{j}]^{-1} & \mathbf{0} & \mathbf{0} \\ \mathbf{0} & \mathbf{0} & \mathbf{I} \end{bmatrix}. \tag{B.13}$$

In frames with many parts, it will certainly happen that the end point of a part $\Omega_i$ shall be rigidly connected not only with an initial point of the next part, but also with an end point of another part, e.g., with the end point of $\Omega_j$ and the initial point of $\Omega_{i+1}$, the dynamic coupling condition (B.8) has to be changed to

$$\mathbf{T}^i(l_i) = -\mathbf{C}_i^{j}\cdot\mathbf{T}^{j}(0) + \mathbf{C}_i^{i+1}\cdot\mathbf{T}^{i+1}(0), \tag{B.14}$$

which gives the changed dynamic coupling matrix

$$\overset{\langle \mathrm{T} \rangle}{\mathbf{C}}{}^{eeb}_{i,j,i+1} = \begin{bmatrix} \mathbf{I} & \mathbf{0} & \mathbf{0} \\ \mathbf{0} & -\mathbf{C}_i^j & \mathbf{C}_i^{i+1} \end{bmatrix}. \tag{B.15}$$

The above system (B.11) with 18 equations has a unique solution if at each of the three endings of this frame structure, i.e., at $x^i = 0$ of $\Omega_i$, at $x^{i+1} = l_{i+1}$ of $\Omega_{i+1}$, at $x^{i+2} = l_{i+2}$ of $\Omega_{i+2}$, three boundary values are prescribed, e.g., $\mathbf{u}^i(0) = 0$ (fixed), $\mathbf{T}^{i+1}(l_{i+1}) = 0$ (free), and $\mathbf{T}^{i+2}(l_{i+2}) = 0$ (free): Then, from the 27 state values in the vector $[\mathbf{x}_0^i, \mathbf{x}_{cr}^{i,i+1,i+2}, \mathbf{x}_l^{i+1}, \mathbf{x}_l^{i+2}]^{\mathrm{T}}$ only 18 are unknown.

## Appendix C. The Convolution Quadrature Method

Firstly developed by Lubich [17,18], the convolution quadrature method numerically approximates a convolution integral

$$y(t) = \int_0^t f(t-\tau)g(\tau)\,\mathrm{d}\tau \to y(n\Delta t) = \sum_{k=0}^{n} \omega_{n-k}(\hat{f}, \Delta t)g(k\Delta t), \quad n = 0, 1, \ldots, N, \tag{C.1}$$

by a quadrature rule whose weights are determined by the Laplace transformed function $\hat{f}$ and a linear multi-step method. Applications to the boundary element method may be found in Ref. [19]. Here, a brief overview of the method is given.

In formula (C.1), the time $t$ is divided in $N$ equal steps $\Delta t$. The weights $\omega_n(\Delta t)$ are the coefficients of the power series

$$\hat{f}\left(\frac{\gamma(z)}{\Delta t}\right) = \sum_{n=0}^{\infty} \omega_n(\hat{f}, \Delta t) z^n, \tag{C.2}$$

with the complex variable $z$. The coefficients of a power series are usually calculated with Cauchy's integral formula. After a polar co-ordinate transformation, this integral is approximated by a trapezoidal rule with $L$ equal steps $2\pi/L$. This leads to

$$\omega_n(\hat{f}, \Delta t) = \frac{1}{2\pi i}\int_{|z|=\mathscr{R}} \hat{f}\left(\frac{\gamma(z)}{\Delta t}\right) z^{-n-1}\,\mathrm{d}z \approx \frac{\mathscr{R}^{-n}}{L}\sum_{\ell=0}^{L-1} \hat{f}\left(\frac{\gamma(\mathscr{R}\mathrm{e}^{\mathrm{i}\ell(2\pi/L)})}{\Delta t}\right)\mathrm{e}^{-\mathrm{i}n\ell(2\pi/L)}, \tag{C.3}$$

where $\mathscr{R}$ is the radius of a circle in the analytical domain of $\hat{f}(z)$.

The function $\gamma(z)$ is the quotient of the characteristic polynomials of the underlying multi-step method, e.g., for a BDF 2, $\gamma(z) = \frac{3}{2} - 2z + \frac{1}{2}z^2$. The used linear multi-step method must be $A(\alpha)$-stable and stable at infinity [18]. Experience shows that the BDF 2 is the best choice [29]. Therefore, it is used in all calculations in this paper.

If one assumes that the values of $\hat{f}(z)$ in Eq. (C.3) are computed with an error bounded by $\varepsilon$, then the choice $L = N$ and $\mathscr{R}^N = \sqrt{\varepsilon}$ yields an error in $\omega_n$ of size $O(\sqrt{\varepsilon})$ [17]. Several tests conducted by the first author lead to the conclusion that the parameter $\varepsilon = 10^{-10}$ is the best choice for the kind of functions dealt with in this paper [30]. The assumption $L = N$ results in $N^2$ coefficients $\omega_n(\Delta t)$ to be calculated. Due to the exponential function at the end of formula (C.3) this can be done very fast using the technique of the fast Fourier transformation (FFT).

## References


[1] S. Timoshenko, D.Y. Young, *Vibration Problems in Engineering*, 3rd Edition, D. van Nostrand, New York, 1961, pp. 329–331.

[2] J. Prescott, Elastic waves and vibrations of thin rods, *Philosophical Magazine* 33 (1942) 703–754.

[3] Ya.S. Uflyand, The propagation of waves in the transverse vibration of bars and plates, *Prikladnaya Matematika I Mekhanika* 12 (1948) 287–300.

[4] B. Dawson, Rotary inertia and shear in beam vibration treated by the Ritz method, *Aeronautical Journal* 72 (1968) 341–344.

[5] H. Kolsky, *Stress Waves in Solids*, Dover Publications, New York, 1963.

[6] E. Esmailzadeh, A.R. Ohadi, Vibration and stability analysis of non-uniform Timoshenko beams under axial and distributed tangential loads, *Journal of Sound and Vibration* 236 (2000) 443–456.

[7] K.K. Kapur, Vibrations of a Timoshenko beam, using a finite element approach, *Journal of the Acoustical Society of America* 40 (1966) 1058–1063.

[8] R.E. Nickel, G.A. Secor, Convergence of consistently derived Timoshenko beam finite elements, *International Journal for Numerical Methods in Engineering* 5 (1972) 243–253.

[9] U. Kolberg, A general mixed finite element for Timoshenko beams, *Communications in Applied Numerical Methods* 3 (1987) 109–114.

[10] B.A. Ovunc, Dynamics of frameworks by continuous mass method, *Computers and Structures* 4 (1974) 1061–1089.

[11] D.E. Beskos, B.A. Boley, Use of dynamic influence coefficients in forced vibration problems with the aid of Laplace transform, *Computers and Structures* 5 (1975) 263–269.

[12] D.E. Beskos, G.V. Narayanan, Dynamic response of frameworks by numerical Laplace transform, *Computer Methods in Applied Mechanics and Engineering* 37 (1983) 289–307.

[13] G. Fairweather, A. Karageorghis, The method of fundamental solutions for elliptic boundary value problems, *Advances in Computational Mathematics* 9 (1998) 69–95.

[14] C.P. Providakis, D.E. Beskos, Dynamic analysis of beams by the boundary element method, *Computers and Structures* 22 (1986) 957–964.

[15] H. Antes, Fundamental solution and integral equations for Timoshenko beams, *Computers and Structures* 81 (2003) 383–396.

[16] N. Ortner, Die Fundamentallösung des Timoshenko- und des Boussinesq-Operators, *Zeitschrift fur Angewandie Mathematik und Mechanik* 68 (1988) 547–553.

[17] C. Lubich, Convolution quadrature and discretized operational calculus. I, *Numerische Mathematik* 52 (1988) 129–145.

[18] C. Lubich, Convolution quadrature and discretized operational calculus. II, *Numerische Mathematik* 52 (1988) 413–425.

[19] M. Schanz, *Wave Propagation in Viscoelastic and Poroelastic Continua*: *A Boundary Element Approach*, Lecture Notes in Applied Mechanics, Springer, Berlin, 2001.

[20] S.P. Timoshenko, *Strength of Materials—Part* 1, 2nd Edition, D. van Nostrand, New York, 1940, pp. 170–171.

[21] G.R. Cowper, The shear coefficient in Timoshenko's beam theory, *Journal of Applied Mechanics, Transactions of American Society of Mechanical Engineers* 33 (1966) 335–340.

[22] R.J. Roark, *Formulas for Stress and Strain*, 3rd Edition, McGraw-Hill, New York, 1954, pp. 119–121.

[23] R.D. Mindlin, H. Deresiewicz, Timoshenko's shear coefficient for flexural vibrations of beams, *Technical Report No. 10*, *ONR Project NR064-388*, Department of Civil Engineering, Columbia University, New York, 1953

[24] L.E. Goodmann, Discussion of paper "Flexural vibrations in uniform beams according to the Timoshenko theory" by R.A. Anderson, *Journal of Applied Mechanics* 21, *Transactions of the American Society of Mechanical Engineers*, 76 (1954) 202–204.

[25] N. Ortner, P. Wagner, Solution of the initial-boundary value problem for the simply supported semi-infinite Timoshenko beam, *Journal of Elasticity* 42 (1996) 217–241.

[26] L. Hörmander, *Linear Partial Differential Operators*, Springer, Berlin, 1963.

[27] A.H.-D. Cheng, H. Antes, On free space Green's function for high order Helmholtz equations, in: S. Kobayashi, N. Nishimura (Eds.), *Boundary Element Methods*, *Proceedings of the IABEM91*, Kyoto, Japan, Springer, Berlin, 1992, pp. 67–71.
[28] K. Knothe, H. Wessels, *Finite Elemente, Eine Einführung für Ingenieure*, Springer, Berlin, 1999.
[29] M. Schanz, A boundary element formulation in time domain for viscoelastic solids, *Communications in Numerical Methods in Engineering* 15 (1999) 799–809.
[30] M. Schanz, H. Antes, Application of 'operational quadrature methods' in time domain boundary element methods, *Meccanica* 32 (3) (1997) 179–186.